ELSEVIER

Biophysical Chemistry 104 (2003) 655–682

Biophysical Chemistry

www.elsevier.com/locate/bpc

The effects of Tubulin denaturation on the characterization of its polymerization behavior☆

Damien Hall*,[1]

Section on Physical Biochemistry, Lab 222, Bld. 8, National Institute of Diabetes, Digestive and Kidney Disease, National Institutes of Health, Bethesda, MD 20892, USA

Received 10 January 2003; received in revised form 10 February 2003; accepted 10 February 2003

Abstract

We report here upon a simulation study examining the effect of a dynamic mode of Tubulin denaturation upon the kinetic and thermodynamic characterization of the polymer formed for two idealized models of a Tubulin polymerization reaction: (i) an irreversibly polymerizing system; and (ii) a reversibly polymerizing system. The effects of each denaturation mode upon the two model systems behavior are highlighted by interpretation of the data in terms of the classical Oosawa reversible condensation polymerization model. We reveal here findings which suggest that the measurement strategy in concert with Tubulin's instability over the time course of the experiment may bias the results obtained so as to make an irreversible system's behavior conform to the equilibrium model or alternatively distort the results obtained from a truly reversible system to produce values of the critical concentration quite seriously in error. It was also found that Tubulin denaturation may seriously distort parameter estimates gained from a kinetic characterization of the system (e.g. nucleus size and growth rate constant).

Keywords: Microtubules; Tubulin denaturation; Kinetics; Thermodynamics; Polymerization

1. Introduction

Tubulin is a protein that exists as an approximately 100,000 Da heterodimer [1] composed of near equivalent subunits termed α and β. Tubulin constitutes the primary building block of the microtubule—a helical tubular polymer that is one of the principle components of the cell cytoskeleton. Tubulin is a primary target for anticancer drug therapy and defects in its mode of action can cause a number of serious disease states [2].

The physical biochemistry of Tubulin constitutes an exceedingly complex system with regards to its polymerization behavior (Tubulin can polymerize to form a plethora of polymer types [3–6]), drug binding (analysis has shown some reversible and irreversible [7,8] as well as quaternary state-specific mechanisms [9]) and in its interaction with

Abbreviations: ODE, ordinary differential equation; GDP, Guanosine-5′-diphosphate; GTP, Guanosine-5′-triphosphate; MT, microtubule.

☆ The US Government has a right to retain a non-exclusive royalty-free license in and to any copyright covering this paper.

*Corresponding author. Tel./fax: +44-1223-763418.

E-mail address: drh32@cam.ac.uk (D. Hall).

[1] Present address: Biophysical Section, Chemistry Department, Cambridge University, Lensfield Rd., Cambridge CB2 1EW, UK.

0301-4622/03/$ - see front matter © 2003 Elsevier Science B.V. All rights reserved.
doi:10.1016/S0301-4622(03)00040-1

nucleotides (both irreversible and reversible binding behavior coupled with nucleotide hydrolysis [10,11]).

The polymerization of Tubulin is generally thought to follow a mechanism based on the condensation growth models of an ordered crystal [12–15]. As such the kinetic characterization (Fig. 1) of Tubulin polymerization has involved parameterizing the time-dependence of polymer formation in terms of a nucleation rate constant (by analysis of the lag time—either an inflection point in the polymer time course or some arbitrary marker such as the tenth time[2] [16–18]), a growth phase association and dissociation rate constant [14,19,20] and an equilibrium or 'steady state' position [12,13,16]. In keeping with the condensation-growth mechanism, the thermodynamic characterization of Tubulin self-association (Fig. 2) has involved measurement of the 'critical concentration' (the reciprocal of the association equilibrium growth constant) by recording the equilibrium solubility of unpolymerized Tubulin from a range of initial starting concentrations with subsequent extrapolation back to apparently zero polymerization.

One major difficulty to gaining reliable data about Tubulin polymerization lies in the fact that Tubulin is an extremely unstable and labile protein [21–23]. The denaturation of Tubulin can be (and has been) considered on many different levels depending on the marker chosen for such assessment. Table 1 represents a compendium of some of the different means available for the consideration of Tubulin denaturation and highlights the functional property measured. Where known Table 1, also lists the appropriate numeric descriptor that characterizes the rate of denaturation of the particular marker in question (under a particular set of solution conditions). Although Tubulin denaturation has been a much considered topic the emphasis has been on studying the aging process at the low temperature conditions associated with storage [22,24–27]. As Tubulin polymerization is a temperature initiated or driven process [28,29], instigation of polymerization usually involves heating the sample from 0 °C to higher temperatures (ranging up to 37 °C). It has been demonstrated previously that the rate of Tubulin denaturation is markedly increased at elevated temperatures [30–32]. Previously, account of Tubulin denaturation during a polymerization assembly assay has been made by assuming a certain percentage of the sample incompetent at zero time and correcting the total Tubulin concentration by subtraction of this factor ([12,13,16,24] and see Fig. 2). However, the effect upon the experimentally recorded profile of a dynamic Tubulin decay process at the elevated temperatures required for assembly has heretofore yet to be considered. In this paper, we explore the effects of such a dynamic decay process by simulating the effect of various hypothesized modes of dynamic Tubulin denaturation. We examine the effects of such dynamic decay upon the kinetics and thermodynamics of Tubulin polymerization in terms of the descriptive parameters (described in Figs. 1 and 2) used for characterization of the system.

2. Theory section

2.1. Idealized model systems of Tubulin polymerization

2.1.1. (i) Reversible model

The condensation–growth model for Tubulin polymerization (Eq. (1)) first involves formation of a thermodynamically unstable nucleus of crystallization, N, from a pool of free monomer[3], M, followed by successive addition of monomer units to form a stable array of high degree polymers ranging from P_1 to P_z where P_z is the largest polymer species in solution [15,33]. Although undoubtedly the situation is more complex than that shown in Eq. (1), we depict the formation of the unfavorable nucleus by a discrete series of second order association reactions and first order dissociation reactions that lead to a species of critical nucleus, N_i, of size, n. For simplicity the rate constants governing each stage in the nucleation process are considered equivalent for the

[2] The time required for the signal to attain one-tenth of its maximum value.

[3] The definition of 'monomer' referring to the $\alpha\beta$ heterodimer of 100,000 molecular weight.

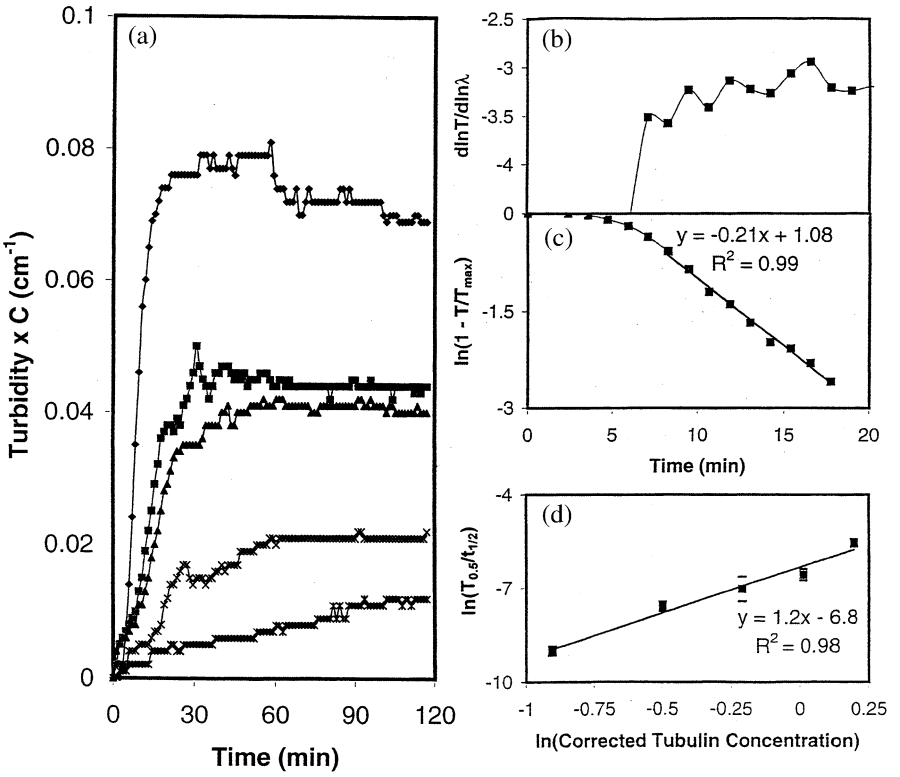

Fig. 1. Demonstration of a typical experimental approach to the kinetic characterization of the Tubulin polymerization reaction. Tubulin isolated from calf brain by the method of thermal cycling [40] and further purified by phosphocellulose chromatography was purchased from the lab of Dr E. Hamel at the NIH. The Tubulin fractions (80 mg/ml) purchased in 0.1 M PIPES, pH 6.9, 1 mM GTP, 1 mM $MgSO_4$, 0.1 mM EGTA, 4 M glycerol were equilibrated into a similar buffer (0.1 M PIPES pH 6.4, 1 mM $MgSO_4$, 0.1 mM EGTA) by passage through a 5×2 cm (length×diameter) sephadex G-25 desalting column (Pharmacia Biotech) at 4 °C. This sample was then centrifuged for 15 min at 4 °C at an average centrifugal field of 10,000×g in an Eppendorf benchtop centrifuge (1.5-ml polyethylene tubes filled with 0.5-ml sample). After isolation of the supernatant and its subsequent concentration determination based on an $E^{1\%}_{1\,cm}$ of 10.4 at 278 nm in 1% SDS [7], the Tubulin solution was made 1 mM in GTP and 150 mg/ml in dextran (Pharmacia, M_w = 10,000 Da). (a) Polymerization of Tubulin as recorded by solution turbidity not normalized for path length at 350 nm (Tubulin solutions at 0.50, 0.75, 1.00, 1.25 and 1.50 mg/ml, bottom to top) in a micromax 96 well plate reader. All wells had the same volume (and therefore same optical path length) and all turbidity curves were recorded simultaneously at six wavelengths (350, 400, 450, 500, 550 and 600 nm). Polymerization was initiated by taking the 96 well plate from 4 to 37 °C by heating for 1 min in a 60 °C water bath. (b) Linear regression of the dependence of the natural logarithm of the turbidity on the natural logarithm of the wavelength for the 1.5 mg/ml sample yielded a slope of approximately −3 after approximately 5 min in accordance with the Berne approximation [12] for treating turbidity as a marker of the weight concentration of Tubulin existing as polymer. This requirement was not met for the other concentrations of Tubulin studied. (c) A first order kinetic plot of the 1.5 mg/ml Tubulin sample showing apparent first order behavior after the first five min. (d) Crude attempt at the examination of the concentration dependence of the initial rate of polymerization as recorded by turbidity. The natural logarithm of the average rate of attainment on the half maximal value of the turbidity vs. the natural logarithm of the corrected Tubulin concentration (see Fig. 2) yields a slope that is usually considered proportional to the average nucleus size [16].

forward, k_{N+}, and reverse directions, k_{N-}. This formulation of the nucleation process is done in the belief that the formulation is at once both simple enough to not detract from the primary focus of the article—the examination of denaturation upon Tubulin polymerization kinetics and thermodynamics, and yet is still preserving of a sufficient physical basis as to have some credulity

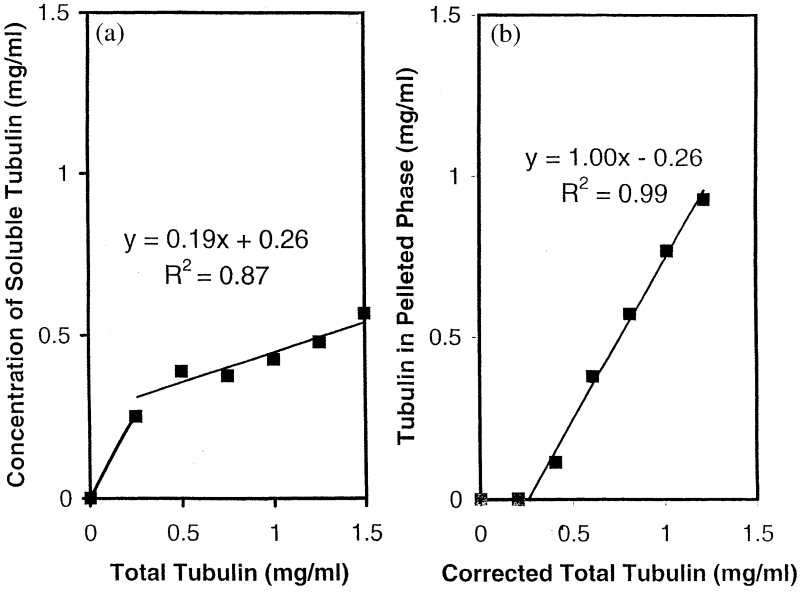

Fig. 2. Demonstration of a typical experimental approach to the thermodynamic characterization of the Tubulin polymerization reaction. In a tandem experiment, the same Tubulin concentrations (plus an additional 0.25-mg/ml sample) in the same buffer conditions as shown in Fig. 1 were allowed to polymerize for 2 h at 37 °C and were then centrifuged at an average of 20,000×g for 30 min at the same temperature (in a Sorvall benchtop centrifuge in 1.5-ml polyethylene eppendorf tubels filled with 0.15 ml sample). The supernatant was removed and the concentration of Tubulin in the pellet was determined by the bicinchonic acid procedure using BSA as a standard [65]. All assays were done in duplicate and the relationship between the concentration estimate from the BCA test and that from the spectrophotometric assay was established previously. (a) Plot of the difference between total Tubulin and the Tubulin in the pellet after centrifugation vs. the total concentration of Tubulin. The positive slope and intercept of the graph could be taken as showing 19% inactive Tubulin and a critical concentration of 0.26 mg/ml. (b) Plot of concentration of Tubulin in the pellet phase vs. the total concentration of Tubulin corrected for a possible 19% inactive component.

to an experimentalist investigating the power dependence of the rate of the nucleation process on Tubulin concentration. The growth step as written in Eq. (1) involves only reversible sequential addition of free Tubulin which is characterized by a second order association constant k_{G+} and a first order dissociation rate constant k_{G-}.

$$
\begin{aligned}
&2\mathrm{M} \underset{k_{N-}}{\overset{k_{N+}}{\rightleftharpoons}} \mathrm{N}_2\\
&\mathrm{N}_2+\mathrm{M} \underset{k_{N-}}{\overset{k_{N+}}{\rightleftharpoons}} \mathrm{N}_3\\
&\quad\cdot\quad\cdot\quad\cdot\\
&\mathrm{N}_i+\mathrm{M} \underset{k_{G-}}{\overset{k_{G+}}{\rightleftharpoons}} \mathrm{P}_1\\
&\mathrm{P}_1+\mathrm{M} \underset{k_{G-}}{\overset{k_{G+}}{\rightleftharpoons}} \mathrm{P}_2\\
&\quad\cdot\quad\cdot\quad\cdot\\
&\mathrm{P}_{z-1}+\mathrm{M} \underset{k_{G-}}{\overset{k_{G+}}{\rightleftharpoons}} \mathrm{P}_z
\end{aligned}
\qquad (1)
$$

A set of interrelated first order differential equations can be written describing the rate of formation of each polymer species. Such a formulation is described by Eq. (2).

$$
\begin{aligned}
d[N_2]/dt &= -k_{N+}[N_2][M]-k_{N-}[N_2]+k_{N+}[M]^2+k_{N-}[N_3]\\
&\quad\cdot\qquad\qquad\cdot\qquad\qquad\cdot\\
d[N_i]/dt &= -k_{G+}[N_i][M]\\
&\quad -k_{N-}[N_i]+k_{N+}[N_{i-1}][M]+k_{G-}[P_1]
\end{aligned}
$$

Table 1
Some means for the consideration of tubulin denaturation

Marker of denaturation	Property lost or gained	Numeric descriptor[a] and solution environment
Polymerization	Inability to reversibly polymerize to high molecular weight polymer	$t_{1/2}$ ~2.5 h (37 °C)[b] $t_{1/2}$ ~0.5 h (37 °C)[c] $t_{1/2}$ ~15 h (4 °C)[b]
	Inability to participate in Taxol-induced irreversible polymerization	$t_{1/2}$ ~5–47 h (20 °C)[d]
Fluorescence	Change in native fluorescence spectrum	$t_{1/2}$ ~25 h (loss of fluorescence at 435 nm, 0.1 mg/ml Tubulin at 4 °C)[e] red shift of emission maximum complete within 50 h (Tubulin at 4 °C)[e]
Colchicine binding	Loss of ability to bind Colchicine	$t_{1/2}$ ~5–70 h loss of uptake of MTC[f] (Tubulin at 20 °C)[d] $t_{1/2}$ ~10 h (37 °C)[b] $t_{1/2}$ ~4 h (0.2 mg/ml Tubulin, 37 °C)[c] $t_{1/2}$ ~11 h (Tubulin at 4 °C)[g] $t_{1/2}$ ~220 h (Tubulin at 4 °C)[h] $t_{1/2}$ ~0.1 h (Tubulin at 60 °C)[i]
Circular dichroism	Changes in CD spectra	Approximately 30% loss of 220 nm signal after 44 h (1 mg/ml Tubulin at 4 °C)[i]
Irreversible aggregate	Appearance of irreversible aggregate that is sensitive to reducing agent	$t_{1/2}$ ~25 h (Tubulin at 4 °C)[b] $t_{1/2}$ ~30 h (Tubulin at 4 °C)[i]
Chemical modification	Formation of isoaspartyl and lysinoalanine bonds and other chemical degradation products	Time span of reaction occurring on the order of 30 days at 37 °C [60,67,68]

[a] Note the referral to a half life does not necessarily imply pseudo-first-order kinetics. The quoted value may also be given in its more general sense of the time taken for the reaction to proceed to one half of its original extent.
[b] 0.1 M PIPES pH 6.5, 1 mM $MgSO_4$, 1 mM EGTA, 1 mM GTP [21].
[c] 0.025 M MES pH 6.55, 1 mM $MgCl_2$, 0.1 mMEDTA, 0.5 mM GTP [41].
[d] 10 mM phosphate pH 7.0, 1 mM EDTA, $MgCl_2$ varied from 60 nM to 1 mM [31].
[e] 10 mM phosphate pH 7.0, 0.1 mM GTP [22].
[f] MTC = 2-methoxy-5-(2,3,4-trimethoxyphenyl)-2,4,6-cycloheptatrien-1-one—A colchicine analog.
[g] 1 mM Tris–HCl, pH 7.0, 1 mM GTP, 10 mM $MgCl_2$ [56].
[h] 1 mM Tris–HCl, pH 7.0, (4 M glycerol or 0.8 M sucrose) 1 mM GTP, 10 mM $MgCl_2$ [56].
[i] 10 mM phosphate pH 7.0, 0.1 mM GTP [26].

$$
\begin{aligned}
d[P_1]/dt &= -k_{G+}[M] \\
&\quad \times [P_1] - k_{G-}[P_1] + k_{G-}[P_2] + k_{G+}[N_i][M] \\
d[P_2]/dt &= -k_{G+}[M] \\
&\quad [P_2] - k_{G-}[P_2] + k_{G-}[P_3] + k_{G+}[P_1][M] \\
&\quad \cdot \qquad \cdot \qquad \cdot \\
d[P_Z]/dt &= -k_{G-}[P_Z] + k_{G+}[P_{z-1}][M] \qquad (2)
\end{aligned}
$$

A microtubule of length 10 μm might contain more than 16,000 individual tubulin monomers (assuming a helical pitch of approximately 9 nm for the microtubule [6]) thereby necessitating that Eq. (2) contain the equivalent number of differential equations. Previously, methods based on approximations have been applied to simplify equation set 2 to only a few differential equations that yield information on the total concentration of polymerized monomer. We have chosen to explicitly model the rate of formation of each chemical species via a simple matrix procedure that is outlined in the appendix.

The growth stage of polymerization can be thought of as consisting of two distinct overall phases. The first phase involves the relatively rapid

attainment of a near or 'pseudo-equilibrium' position with regards to soluble monomer in exchange with polymer species. The second relatively slow phase involves the redistribution of polymer lengths and the attainment of a final or 'true' equilibrium position.[4] At long times, the behavior predicted by numerical integration of equation set 2 will yield the equilibrium distribution. However, a much more direct method of defining the equilibrium distribution involves consideration of Eq. (1) in terms of the law of mass action. Such consideration yields the equilibrium relation defining the composition of the total concentration of monomer species, $[M]_{\mathrm{tot}}$.

$$[M]_{\mathrm{tot}} = \sum [P]_{\mathrm{eqm}} + \sum [N]_{\mathrm{eqm}} + [M]_{\mathrm{eqm}}$$

$$\sum [P]_{\mathrm{eqm}} = (K_N)^{\mathrm{i}} l \sum_{l=1}^{z} l (K_G)^{(l-i)} [M]_{\mathrm{eqm}}^{1}$$

$$\sum [N]_{\mathrm{eqm}} = \left(\sum_{j=1}^{\mathrm{i}=1} (j+1)(K_N)^{j} [M]^{(j+1)} \right) \qquad (3)$$

where $\sum [N]_{\mathrm{eqm}}$ is the equivalent concentration of monomer existing as nuclei and pre-nucleus fragments, $\sum [P]_{\mathrm{eqm}}$ is the concentration of monomer existing as growth polymer (i.e. degree > nucleus size) and $[M]_{\mathrm{eqm}}$ is the equilibrium concentration of monomer.

2.1.2. (ii) Irreversible model

As a result of the action of certain drugs (e.g. Taxol), the growth steps of the polymerization process is thought to become irreversible [34]. To simulate the early to intermediate times of irreversible polymerization of Tubulin we have set k_{G-} in Eq. (2) to zero. As an additional check on the system we have resorted to a description (Eq. (4)) concerned only with the free concentration of monomer, nuclei, polymer ends $[E]$ and total concentration of monomer within all polymer species $[p]_{\mathrm{tot}}$. The rate of formation of polymer ends capable of sustaining further polymer growth is obtained via the summation of all rate equations describing species of degree greater than the critical nucleus size [15]. Although such a formulation provides no information on the length distribution of the polymer produced, it avoids the gigantic matrix sizes associated with the extremely long polymers associated with the irreversibility constraint.

$$d[E]/dt = k_{N+}[N_{\mathrm{i}-1}][M] - k_{N-}[N_{\mathrm{i}}]$$

$$d[p]_{\mathrm{tot}}/dt = k_{G+}[E][M] + (i-1)k_{G+}[N_{\mathrm{i}}][M]$$

$$d[N_2]/dt = k_{N+}[M]^2 - k_{N-}[N_2] - k_{N+}[N_2][M] + k_{N-}[N_3]$$

$$d[N_{\mathrm{i}}]/dt = k_{N+}[N_{\mathrm{i}-1}][M] - k_{N-}[N_{\mathrm{i}}] - k_{G+}[N_{\mathrm{i}}][M]$$

$$d[M]/dt = -\left(d[p]_{\mathrm{tot}}/dt + \sum_{z=2}^{\mathrm{i}} z\, d[N_2]/dt \right) \qquad (4)$$

Unlike the reversible case the growth phase of the irreversible polymerization process does not reorganize to attain an equilibrium length distribution but rather proceeds to an irreversible end point and therefore is not characterized by a slow redistribution phase.

2.1.3. (iii) Simple kinetic analysis

Two general approaches have been attempted for deriving the kinetic rate constants relating to the growth step in Tubulin polymerization: (i) graphical analysis in terms of a pseudo-first order transform [14,19,20]; and (ii) non-linear least squares fitting to an approximate expression [16,18,35].

As we have the luxury of a defined mechanism and error free data here we opt for the simpler of the two methods and choose graphical analysis for the presentation of our simulated results. The graphical method evolves from conceptualization of the polymerization reaction in terms of the following two differential rate expressions:

$$d[E]/dt = k_{N+}[N_{\mathrm{i}-1}][M] - k_{N-}[N_{\mathrm{i}}]$$

$$d[p]_{\mathrm{tot}}/dt = k_{G+}[E][M] + (i-1)k_{G+}[N_{\mathrm{i}}] \times [M] - k_{G-}\left([E] + i[P_1] - [N_{\mathrm{i}}]\right) \qquad (5)$$

[4] In the discussion, we will address the validity of considering a process that involves GTP hydrolysis in terms of equilibrium arguments.

For this analysis to succeed one must assume: (a) that at sufficiently long times the change in the concentration of ends is so small as to allow this to be considered a constant; (b) that the concentration of free Tubulin can be calculated as the difference between total Tubulin and Tubulin present within polymer ($[M] \sim [M]_{tot} - [p]_{tot}$); and (c) the concentration of the number of critical nuclei is small in comparison to the concentration of ends i.e. $[E] \sim [E] - [N_i]$. These three assumptions allow us to integrate the bottom equation of Eq. (5), which upon rearrangement yields:

$$\ln\left\{1 - [p]_{tot}/\left([p]_{tot}\right)_{max}\right\} \cong -k_{G+}[E]t \quad (6)$$

where t and $([p]_{tot})_{max}$ describe the elapsed time and the end point equivalent concentration of Tubulin monomers existing as microtubules. Therefore, a plot of $\ln\{1 - [p]_{tot}/([p]_{tot})_{max}\}$ vs. time produces a graph with a slope equal to $-k_{G+}[E]$.

2.2. Tubulin denaturation

Confusion about the rate of Tubulin 'denaturation' is partly brought about by the use of: (i) different arbiters of native structure/activity ([23] and see Table 1); (ii) differences in the effects of the solution environment (e.g. temperature, pressure and composition) on the particular marker of assessment chosen for the study [36,37]; and (iii) the nature of the Tubulin used (e.g. purified Tubulin, modified Tubulin, or Tubulin in association with MAPS [38]).

If we assume that the form of Tubulin that corresponds to the loss of each marker described in Table 1 represents a distinguishable state then one could envisage a simple minimal scheme for the denaturation mechanism of Tubulin involving a progression (reversible or otherwise) from native Tubulin through each of the intermediate species, in order of their rate of attainment, to the final distinguishable species. Such a 'local unfolding' model has been previously suggested by Sackett et al. [23] on the basis of their measurement of a number of Tubulin denaturation markers at varied urea concentrations. In this paper, we are concerned only with how denaturation effects the polymerization behavior of Tubulin and, therefore, we will restrict ourselves to general models of denaturation that focus only on polymerization as the marker of activity. Two assumptions will be implicit in all modeling presented throughout this investigation. The first assumption is that there exists a measurement strategy that is able to continuously and precisely determine the mass distribution of the polymerized material in a manner sufficient to distinguish polymer from non-polymer species. This assumption is met to a certain extent by measurement techniques based on sedimentation and light scattering [39]. The second assumption is that the Tubulin denaturation rate constant exists as a discontinuous step function over the quaternary state of Tubulin. Put more simply, this assumption means that the monomer undergoes denaturation governed by a finite rate constant, whereas the rate constant for the monomer incorporated into the polymer becomes zero. This second assumption finds support in common experimental practice which relies upon the integrity of Tubulin monomers re-purified from Microtubules [40].

We will consider two specific models founded in either of two broad classes of Tubulin denaturation modes.

(i) irreversible first order decay of Tubulin monomer to non-polymerizable monomer, M^*, characterized by a first order rate constant k_{den} [31,41]:

$$M \xrightarrow{k_{den}} M^* \quad (7)$$

(ii) A reversible decay of Tubulin monomer to non-polymerizable monomer, M^* governed by an equilibrium constant K_{DEN}, followed by a sequence of irreversible second order reactions between denatured and native Tubulin monomers to form a polydisperse aggregate, Ag_i of degree i [21,22,42]. The second order rate constant governing this process is denoted k_{*+}. For simplicity we have set all aggregation second order rate constants to a common value although this need not necessarily be the case.

$$M \overset{K_{DEN}}{\rightleftharpoons} M^*(+M) \overset{k_{*+}}{\rightarrow} Ag_1(+M) \overset{k_{*+}}{\rightarrow} Ag_2(+M) \overset{k_{*+}}{\rightarrow} \ldots \rightarrow Ag_i \quad (8)$$

2.3. Parameter selection

A standard Tubulin characterization experiment involves monitoring the polymerization of initial free Tubulin at concentrations between 0 and 2 mg/ml (approximately 0–20 μM). The characteristic time span of the assay [6,14] stretches quite markedly with small variations in Tubulin concentration typically from several hours at the lower concentrations to a matter of minutes at the upper concentrations. Values for the growth rate constants $k_{g+}=2\times10^6$ M^{-1} s^{-1} and $k_{g-}=10$ s^{-1} ($K_G=2\times10^5$ M^{-1}—a critical concentration of approximately 0.5 mg/ml) have been chosen so as to conform to experimental measurement (see discussion [14,33,43]).

Values for the nucleation rate constants have been a little more difficult to ascribe. The mechanism of nucleation presented in the Section 2 does not describe the true complexities of the microtubule nucleation process which may very well be an intrinsically variable process [16,44]. As the aim of the present exercise was to see how denaturation of the Tubulin monomer affects the characterization of a polymerization assay we have set the nucleation rate constants in our model with an eye to producing the characteristic time behavior that is observed experimentally, i.e. the minutes to hour time courses over the experimental concentration range. However, a number of additional constraints were imposed on the selection, namely:

i. That the nucleation dissociation rate constant was greater than the growth dissociation rate constant ($k_{N-}>k_{G-}$ therefore $k_{N-}>10$ s^{-1}).[5]
ii. The nucleation equilibrium constant was less than 1% of the growth equilibrium constant ($K_N \le K_G/100$) so as to conform to the requirements of a true nucleated condensation model (therefore $K_N<2\times10^3$ M^{-1}).
iii. That the nucleation association rate constant is less than the growth association constant ($k_{N+}<k_{G+}$ therefore $k_{N+}<2\times10^6$ M^{-1} s^{-1}).
iv. That the association rate constant (k_{N+}) should not be of such a small magnitude that nucleus formation was kinetically rather than thermodynamically rate limited.

These considerations resulted in the choice of $k_{N-}=500$ s^{-1} and $k_{N+}=5\times10^3$ M^{-1} s^{-1} for the nucleation dissociation and association rate constants (therefore $K_N=10$ M^{-1}). The nucleus size has been fixed at 3.

For the case of simple first order decay the denaturation rate constants have been inferred directly from experiment (listed in Table 1) with the lower and upper bounds of k_{den} equal to 0.8×10^{-4} s^{-1} and 4×10^{-4} s^{-1}, respectively. For the model involving a second order rate-dependence of decay upon Tubulin concentration the parameters have been deduced from experiment in a more indirect fashion. The initial equilibrium between active and inactive Tubulin is considered to be so rapid as to be instantaneous [21,42]. The value of the association equilibrium constant K_{DEN} has been set at 0.1 such that at any time approximately 10% of all monomeric Tubulin exists in the partially denatured form *M**. This seemingly large value was chosen to account for the observation that Tubulin, which was unable to polymerize but had yet to undergo significant irreversible aggregation, could be re-natured by the addition of either D_2O [21] or removal of the denaturant [45]. In both studies, the rescued Tubulin was a demonstrable fraction (i.e. > 10%) of the total concentration—thus justifying, to some extent, our rather large chosen value of 0.1 for K_{DEN}. Determination of a numerical value for the second order denaturation rate constant k_{*+} involved solution of equation set 9 with the imposed boundary condition $[M]=([M]_{tot})/2$ at the specified half life taken from Table 1.

$$[M^*]=K_{DEN}\left([M]_{tot}-[Ag]_{tot}-[p]_{tot}\right)/(1+K_{DEN}) \quad (9a)$$

[5] We feel that our selection of a $k_{N-}>k_{G-}$ is valid in the sense that dissociation of monomer from a single contact point (lateral or longitudinal) should be faster than dissociation of a monomer bonded to its neighboring molecules in the microtubule lattice (at both lateral and longitudinal contact sites [6]) on the grounds of a simple chelate effect.

$$d[\mathrm{AgEnds}]/dt = k_{g+}[M^*][M] \quad (9b)$$

$$d[\mathrm{Ag}]_{tot}/dt = k_{g+}(2[M^*] + [\mathrm{AgEnds}])[M] \quad (9c)$$

$$[M] = [M]_{tot} - [\mathrm{Ag}]_{tot} - [M^*] - [p]_{tot} \quad (9d)$$

where $[\mathrm{Ag}]_{tot}$ is defined as the equivalent concentration of Tubulin monomer existing as irreversible aggregate and [AgEnds] is the molar concentration of aggregate species.

We note that for this mode of denaturation to exhibit a half life of approximately 2.4 h at an initial free Tubulin concentration of 2 mg/ml [21], a value for k_{*+} of 17.5 M^{-1} s^{-1} is required. So as to get some feel for the effect of an increase in the denaturation rate constant on the rate of Microtubule formation, we have selected a value five times that inferred from the data of Chakrabarti et al. [21], $k_{*+} = 87.5$ M^{-1} s^{-1}, a selection in keeping with the fivefold variation in the first order denaturation rate explored in the simpler of the two denaturation models.

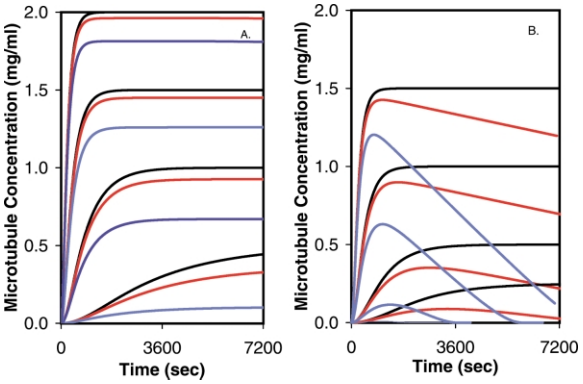

Fig. 3. Simulation of the kinetics of polymerization in which Tubulin monomer may denature by a first order mechanism. Effect on (A) an irreversible system at total Tubulin concentrations of 0.5, 1.0, 1.5 and 2.0 mg/ml and (B) a reversible system at total Tubulin concentrations of 0.75, 1.0, 1.5 and 2.0 mg/ml. Red lines indicate low estimate of $k_{den} = 0.8 \times 10^{-4}$ s^{-1}, blue lines indicate high estimate of $k_{den} = 4.0 \times 10^{-4} s^{-1}$. Black lines show original stable case. Input parameters $k_{N+} =$ 5000 M^{-1} s^{-1}, k_{N-} 500 s^{-1}, $k_{G+} = 2 \times 10^6$ M^{-1} s^{-1}, $n = 3$, $k_{G-} = 0$ s^{-1} (irreversible case), $k_{G-} = 10$ s^{-1} (reversible case).

3. Results

3.1. Effect of denaturation on polymer formation

3.1.1. Case one: denaturation occurring via a first order mechanism

In this section we examine the effect of a first order decay of Tubulin monomer (Eq. (7)) on the kinetic and thermodynamic characterization of polymerization. In the following diagrams we depict the computed effects of a slow denaturation rate of monomer (red line) and a fast denaturation rate of monomer (blue line) on each of the characterization strategies evinced in the previous section. In order to make apparent the effect of Tubulin denaturation on the polymerization characterization, we contrast these results against the case of no denaturation of monomer (i.e. Tubulin completely stable) which is shown as a black line.

Fig. 3A,B shows the respective simulated behavior of the irreversible and reversible polymerization reactions over a 2-h experimental window. We note that for the reversible reaction denaturation leads to a non-stable reaction maximum. However, this is not the situation for the irreversible case (for the reversible case the polymerization of 0.75 mg/ml Tubulin undergoing rapid denaturation is not observable as it is coincident with the abscissa). Fig. 4A describes the dependence of the time required for attainment of 95% of the irreversible end point for Tubulin upon the total Tubulin monomer concentration and Fig. 4B describes the time required for attainment of 95% of the monomer–polymer reversible equilibrium position upon total Tubulin concentration. A common feature to note from both the reversible and irreversible systems for which no denaturation is occurring is the double logarithmic-dependence (see inset) of the time required for reaction completion upon monomer concentration. Such a dependence necessarily implies that the time scales for completion of the polymerization experiment increase greatly with decreasing Tubulin concentration. We note that the unstable systems seem to attain their end points (irreversible case) or polymerization maximum (reversible case) more rapidly with increasing rates of denaturation. This point is highlighted by the curvature of the double logarithmic plot shown in the inset.

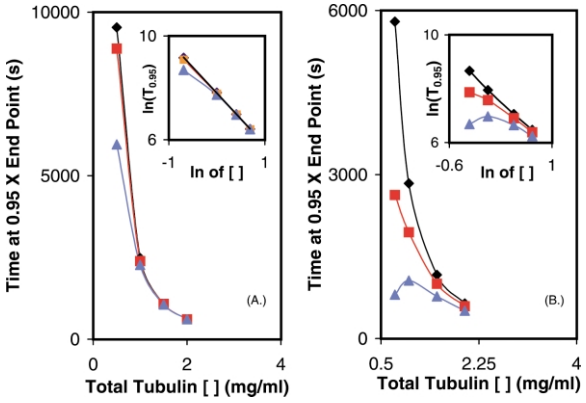

Fig. 4. Effect of a first order denaturation of Tubulin monomer on the relationship between the 95% attainment of an endpoint and the initial Tubulin concentration. (A) The effect of a first order denaturation of the monomer on the irreversibly polymerizing system is minimal with some slight curvature introduced into the log log plot (inset). (B) The effect of a first order denaturation of monomer on the reversibly polymerizing system is pronounced with a significant flattening of the log log plot as the decay rate of the Tubulin monomer is increased. Red lines indicate simulations using low estimate of $k_{den} = 0.8 \times 10^{-4}\ s^{-1}$, blue lines indicate simulations using high estimate of $k_{den} = 4.0 \times 10^{-4}\ s^{-1}$. Black lines show original stable case.

If the experimental assays were performed over the entire Tubulin concentration series such that each concentration was allowed sufficient time to attain its end point or polymerization maximum then the resulting polymer mixture might be separated by ultracentrifugation into soluble and pellet phases. The results of such a hypothetical experiment have been simulated for both irreversible and reversible representations of Tubulin's polymerization behavior and are, respectively, shown in Fig. 5A,B. Note that for the irreversibly polymerizing system which is completely stable (Fig. 5A, black lines) no Tubulin exists in the soluble phase as all Tubulin monomer has been incorporated into the pellet phase, as evidenced by an abscissa intercept of 0 μM. For the irreversible case with first-order denaturation of the monomer, we see that a slow rate of denaturation leads to an assessment of 0.15 (±0.03) mg/ml ($R^2 = 1.0$, slope = 1.07) for the critical concentration. A fast rate of denaturation results in a critical concentration of 0.41 (±0.02) mg/ml ($R^2 = 1.0$, slope = 1.14). Separation of the reaction mixture, of the simulated stable reversible polymerizing system, into polymer and monomer constituents (Fig. 5B, black lines) reveals behavior consistent with an ideal first order phase transition, with a critical concentration of 5 μM (~0.5 mg/ml). The corresponding values for the critical concentration emanating from the simulations for the reversible case susceptible to denaturation were 0.67 (±0.01) mg/ml ($R^2 = 1.0$, slope = 1.07) for the slow denaturation rate and 0.81 (±0.19) mg/ml ($R^2 = 1.0$, slope = 0.98) for the fast denaturation rate.

Fig. 6A,B displays the characterization of the initial lag kinetics via a plot of the log of the rate at the tenth time point (one-tenth of the maximum attained value) for the irreversible and reversible

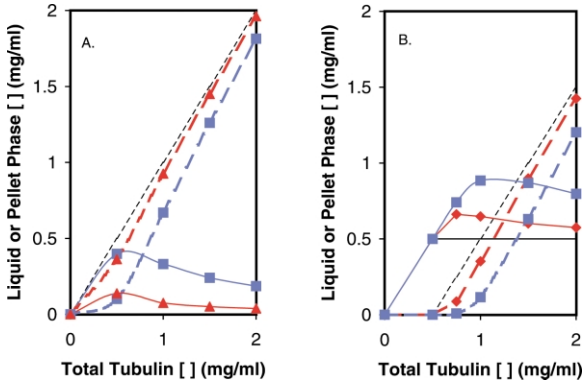

Fig. 5. Effect of denaturation of Tubulin monomer by a first order mechanism on the thermodynamic characterization. The microtubule phase is represented by a dashed line (---) whereas monomer phase is represented by a solid line (—). (A) Irreversibly polymerizing system; (B) reversibly polymerizing system. Black lines show original stable case. Red lines indicate simulations using low estimate of $k_{den} = 0.8 \times 10^{-4}\ s^{-1}$, blue lines indicate simulations using high estimate of $k_{den} = 4.0 \times 10^{-4}\ s^{-1}$. All simulated data points refer to the maximum value obtained from the polymerization profile recorded in Fig. 3. No denaturation, irreversible and reversible systems, respectively, have apparent critical concentrations of 0 and 0.5 mg/ml. The effect of a first order denaturation of Tubulin monomer on the polymerization reaction leads, respectively, to artificial estimates of the critical concentration of: 0.15 (±0.03) mg/ml and 0.41(±0.02) mg/ml for the (A) irreversible system; and 0.67 (±0.01) and 0.81 (±0.19) mg/ml for (B) reversible system (the two estimates, respectively, corresponding to the low and high estimates of the denaturation rate).

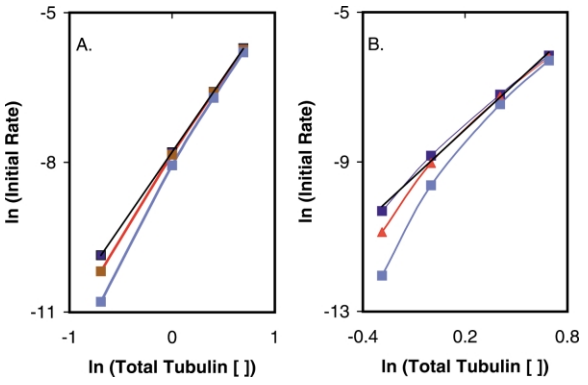

Fig. 6. Effect of denaturation of Tubulin monomer by a first order mechanism on the characterization of the lag phase kinetics. Plot of the natural logarithm of the average initial rate at the tenth time of polymerization vs. the natural logarithm of the total Tubulin concentration. (A) Irreversibly polymerizing system. No denaturation slope yields the input nucleus size of three exactly. Increasing denaturation rate makes more steep the slope of the log log plot of initial rate vs. total Tubulin concentration leading to erroneous estimates of 3.21 ($\pm$0.07) and 3.62 ($\pm$0.13) for the apparent nucleus size. (B) Reversibly polymerizing system. No denaturation, initial rate plot shows an overestimate of the apparent nucleus size at the lower Tubulin concentrations. An estimate closer to three is approached as the Tubulin concentration increases. Increasing the denaturation rate upon the reversible system causes the slope to increase more sharply leading to estimates of 4.70 ($\pm$0.39) and 5.79 ($\pm$0.60) for the two cases. (Red lines $k_{den}=0.8\times10^{-4}$ s^{-1}, blue lines $k_{den}=4.0\times10^{-4}$ s^{-1} and black lines original stable case for comparison).

processes, respectively. For the irreversible polymerization reaction the slope for the completely stable case [slope = 2.96 ($\pm$0.01)] of the logarithmic initial rate plot (black lines) corresponds well with the simulation input nucleus size of 3. However, we note that for the reversible system the slope of the transformed plot for the completely stable case (black line) does not relate simply to the inputted nucleus size with the slope varying from 5.2 at the low concentration end to 3.5 at the highest concentration regime [average slope = 4.21 ($\pm$0.21)]. For both irreversible and reversible cases we observe that the greater the rate of the first order decay process the greater the degree of curvature of the log log relationship and the greater the magnitude of the slope. For the irreversible case the slope of the line increases from 2.96 to 3.21 ($\pm$0.07) and 3.62 ($\pm$0.13) for the slow and fast denaturation rate cases, respectively. For the reversible case the slope increases from 4.21 for the completely stable Tubulin monomer case to 4.70 ($\pm$0.39) and 5.79 ($\pm$0.60) for the slow, and fast denaturation rate cases.

The black lines in Fig. 7A,B describe the logarithmic pseudo-first-order transforms of the irreversible and reversible polymerization time course data, respectively, of Tubulin at 1 mg/ml. With knowledge of the concentration of polymer ends (see bottom of Fig. 7A $[E]_{1\ mg/ml}=0.696$ nM and Fig. 7B $[E]_{1\ mg/ml}=0.676$ nM) the value returned for the association growth rate constants for the stable systems were – irreversible $k_{G+}=2.0\times10^{6}$ M^{-1} s^{-1} and reversible $k_{G+}=1.9\times10^{6}$ M^{-1} s^{-1} (cf. input value of 2.0×10^{6} M^{-1} s^{-1}). For the

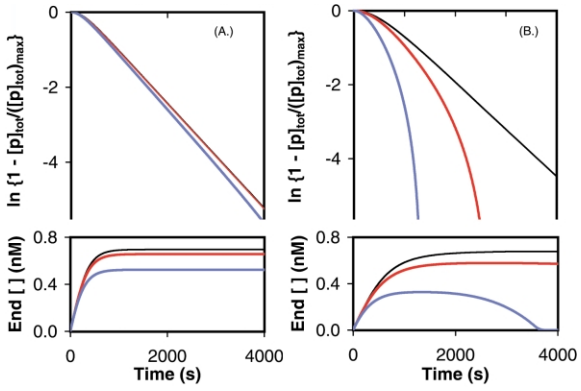

Fig. 7. Effect of denaturation of Tubulin monomer by a first order mechanism on the characterization of the growth phase kinetics. A pseudo-first order kinetic plot of the polymerization of Tubulin in accordance with Eq. (7) (upper panel) and the molar concentration of growing polymer ends ~molar concentration of polymer (lower panel). (A) Characterization of the 1 mg/ml irreversibly polymerizing sample from Fig. 3A. For the stable case evaluation of the limiting slope from the first order kinetic plot in combination with the molar concentration of polymers yields an estimate of $k_{G+}=2\times10^{6}$ M^{-1} s^{-1} (same as input value). With denaturation $k_{G+}=2.1\times10^{6}$ M^{-1} s^{-1} (slow denaturation rate) and $k_{G+}=2.8\times10^{6}$ M^{-1} s^{-1} (fast denaturation rate). (B) Characterization of the 1 mg/ml reversibly polymerizing sample from Fig. 3B. For the stable case similar treatment as in (A) yields an estimate of $k_{G+}=1.9\times10^{6}$ M^{-1} s^{-1}. (cf. input value of $k_{G+}=2\times10^{6}$ M^{-1} s^{-1}). With denaturation $k_{G+}=8.82$ ($\pm$0.12)$\times10^{6}$ M^{-1} s^{-1} (slow denaturation rate) and $k_{G+}=3.84$ ($\pm$0.10)$\times10^{7}$ M^{-1} s^{-1} (fast denaturation rate)

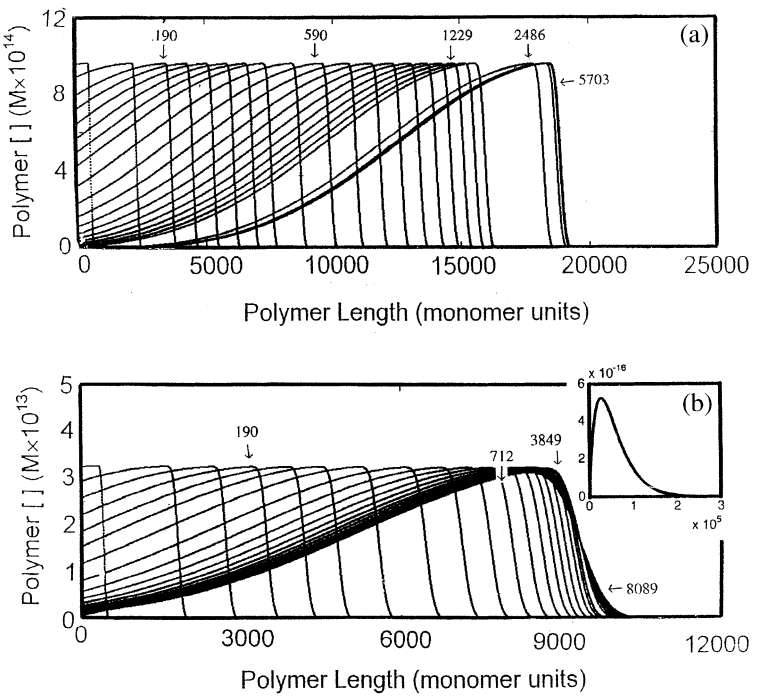

Fig. 8. Examination of the kinetics of the microtubule polymer length distribution resulting from the simulated polymerization of stable Tubulin in Fig. 3. Length distribution of the: (a) 1.0 mg/ml irreversibly polymerizing sample at the marked times (seconds); (b) the 1.5 mg/ml reversibly polymerizing sample. Inset represents the final equilibrium position predicted by Eq. (3) for a system at both polymer mass and length equilibrium.

irreversible case with denaturation, evaluation of the slope of the linear portion of each pseudo-first-order rate plot (slow denaturation slope (2000–2500 s) = 0.00139 ($\pm 1\times10^{-9}$) s^{-1}, fast denaturation slope (2000–2500 s) = 0.00146 ($\pm 8\times10^{-8}$) s^{-1}) together with knowledge of the number concentration of polymer species (lower section Fig. 6A) over the time in question (slow denaturation $[E]_{1\ mg/ml} = 0.657$ nM, fast denaturation $[E]_{1\ mg/ml} = 0.524$ nM) provides estimates of the association growth rate constant of $k_{G+} = 2.1$ (± 0.000002)$\times10^6$ M^{-1} s^{-1} (with slow denaturation of monomer) and $k_{G+} = 2.8$ (± 0.0002)$\times10^6$ M^{-1} s^{-1} (with fast denaturation of monomer) for the irreversibly polymerizing system. For the reversibly polymerizing system undergoing denaturation determination of the slope by linear regression of the pseudo-first-order rate plot over the periods corresponding to stable and maximal concentration of ends [slow denaturation slope (2000–2500 s) = 0.00508 ($\pm 7\times10^{-5}$) s^{-1} $[E]_{1\ mg/ml} = 0.576$ nM, fast denaturation slope (1000–1300 s) = 0.01260 ($\pm 3\times10^{-4}$) s^{-1} $[E]_{1\ mg/ml} = 0.328$ nM] gives estimates of the association growth rate constant of $k_{G+} = 8.82$ (± 0.12)$\times10^6$ M^{-1} s^{-1} (with slow denaturation of monomer) and $k_{G+} = 3.84$ (± 0.10)$\times10^7$ M^{-1} s^{-1} (with fast denaturation of monomer).

The predicted time evolution of the polymer length distributions for the stable irreversible (Fig. 8a, Tubulin concentration = 1 mg/ml) and reversible (Fig. 8b, Tubulin concentration = 1.5 mg/ml) systems resemble each other in general shape and form over the 2-h time period of the hypothetical experiment. For the rate constants utilized in this simulation exercise, polymer formation for the system mimicking Taxol-induced polymerization (irreversible polymerization) proceeds with a very steep front on the advancing side of the polymer length distribution and a gently sloping receding

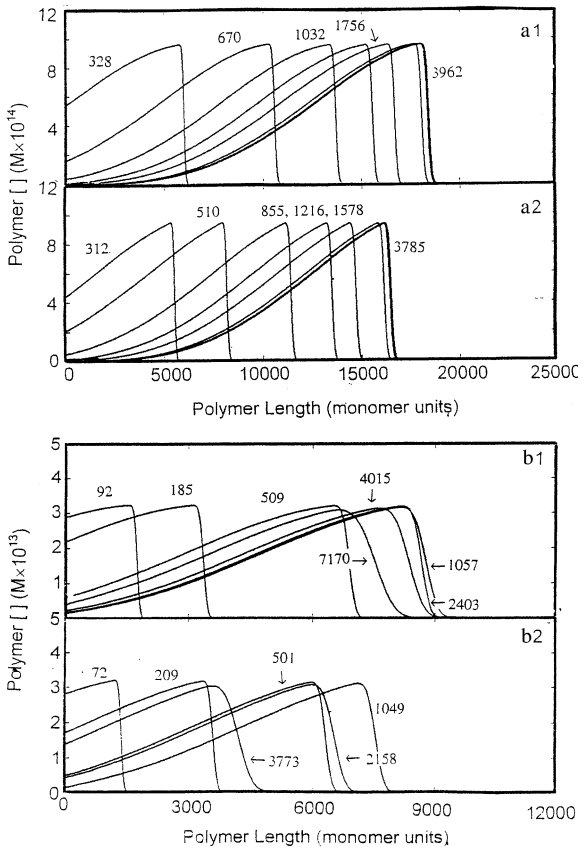

Fig. 9. Examination of the effect of denaturation of the Tubulin monomer by a first order mechanism on the kinetics of the microtubule polymer length distribution. (a) Length distribution of the 1.0 mg/ml irreversibly polymerizing sample at a low (a1) and high denaturation rates. (a2) 1.5 mg/ml reversibly polymerizing sample at low (b1) and high denaturation rates (b2). Arrows indicate time distribution snapshot was taken.

tail. The asymmetry of the advancing polymer front therefore requires that the polymerized monomer predominantly exists within the higher degree polymer species. The weight average molecular weight of the final polymer distribution is 15161 M_M (where M_M is the relative molecular mass of the Tubulin heterodimer ~100,000 Da). With the passage of much time (well outside that which is attainable by the method used for the numerical solution of the differential equation set within the restrictions of this mechanism), the reversible distribution relaxes via a process involving monomer detachment from, and reattachment to the microtubule ends to produce its equilibrium distribution (Eq. (3)). A result of the length redistribution process is a shift of the weight average degree of polymerization to a much larger value, in this instance the average shifts from 7140 M_M at the 2-h period to a massive 56,286 monomer units.

The effect of a first order decay of Tubulin monomer on the simulated time evolution of the polymer length distributions is shown in Fig. 9. For the irreversible polymerization mode (Fig. 9a, Tubulin concentration = 1 mg/ml) the effect of increasing rate of denaturation of the monomer is to retard the length distribution such that the end point distributions for the slow and fast denaturation cases, respectively, have weight average molecular weight of 14811 and 13391 M_M. The simulated effect of increasing the rate of first order denaturation of monomer upon the reversible Tubulin polymerization process (Fig. 9b, Tubulin concentration = 1.5 mg/ml) is such that it limits the maximum attainable size of the distribution and causes the distribution to shrink as the total mass of Tubulin as microtubules begins to decrease. The maximum weight average molecular weights attained by the reversibly polymerizing system when subject to slow, and rapid denaturation of the Tubulin monomer were 6531 and 5696 M_M. An additional point to note from Fig. 9b is the apparent broadening of the distribution, relative to its size, as it shrinks from its maximal length distribution due to denaturation of monomer in solution.

3.1.2. Case two: denaturation occurring via a concentration-dependent mechanism

In case two we explore, via simulation, the effects of a concentration-dependent decay of Tubulin monomer (Eqs. (9a), (9b), (9c) and (9d)) on the kinetic and thermodynamic characterization of Tubulin polymerization. As in case one, we show a slow denaturation rate of monomer (red line), a fast denaturation rate of monomer (blue line) contrasted against no denaturation of monomer (black line).

In Fig. 10, we see the kinetic curves simulating Tubulin polymerization in which the Tubulin monomer is allowed to decay via a second order

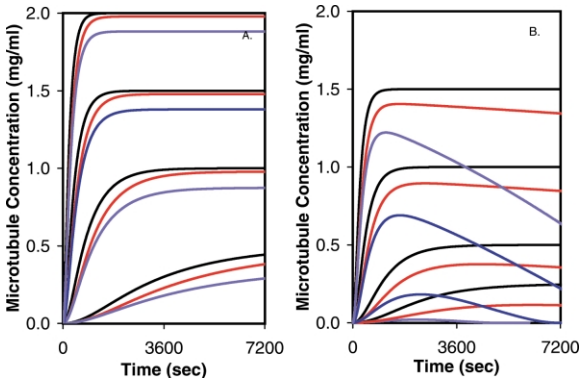

Fig. 10. Simulation of the kinetics of polymerization where Tubulin monomer may denature by a concentration-dependent mechanism. Effect on (A) an irreversible system at total Tubulin concentrations of 0.5, 1.0, 1.5 and 2.0 mg/ml; and (B) a reversible system at total Tubulin concentrations of 0.75, 1.0, 1.5 and 2.0 mg/ml. For both cases $K_{DEN}=0.1$, $k_{*+}=17.5$ M^{-1} s^{-1} (low estimate red line) and $k_{*+}=87.5$ M^{-1} s^{-1} (high estimate blue line). Black lines show original stable case for comparison. Other input parameters $k_{N+}=5000$ M^{-1} s^{-1}, $k_{N-}500$ $s^{-1}=500$ $k_{G+}=2\times10^{6}$ M^{-1} s^{-1}, $n=3$, $k_{G-}=0$ s^{-1} (irreversible case), $k_{G-}=10$ s^{-1} (reversible case).

mechanism. For both the irreversible (k_{G-} set equal to 0 s^{-1}, Fig. 10A) and reversible polymerization cases (k_{G-} set equal to 10 s^{-1}, Fig. 10B) we see that both the lower and upper estimates of the denaturation rate result in demonstrable decreases in the maximal extent of microtubule polymerization. With regard to the irreversible case (Fig. 10A), we note that the end point is delayed rather than advanced, contrary to the corresponding examples shown in case one. For the reversible polymerization case (Fig. 10B) we observe similar reductions in the attained reaction maximum for the higher concentration series (1.5 and 2 mg/ml) when compared to the results from the first order model explored in case one. However, this equivalence is not extended to the lower concentration series for which a higher polymerization maximum is attained in the second case relative to case one.

Fig. 11 describes the effects of a concentration-dependent Tubulin decay process on the attainment of 95% of the end point (irreversible polymerization Fig. 11A) or 95% of the equilibrium position (reversible polymerization Fig. 11B). For both cases, we observe that the behavior is complex. For the irreversible case we see that the curve showing the influence of the slower denaturation rate falls well above the stable monomer case. The curve showing the influence of the faster denaturation rate also lies above both the stable and slow denaturation curves at the high end of the protein concentration range (2 mg/ml) but then crosses the slow denaturation curve at approximately the 1 mg/ml mark. A similar, but more exaggerated trend in behavior is observed in Fig. 11B for the reversible polymerization case. At 2 mg/ml the time required to attain 95% of the equilibrium position is initially greater for both cases reflecting different rates of monomer breakdown than for the stable monomer case. However, with decreasing total Tubulin concentration the time required to reach the near maximal end point position decreases with increasing denaturation rate resulting in an intersection of lines between the curves reflecting denaturation and the stable case. Such behavior

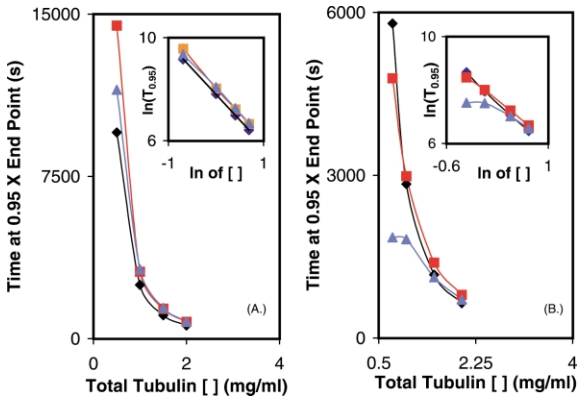

Fig. 11. Effect of a concentration-dependent denaturation mechanism of Tubulin monomer on the relationship between the 95% attainment of an endpoint and the initial Tubulin concentration. (A) The effect of a concentration-dependent mode of monomer denaturation on the irreversibly polymerizing system is minimal with the dependence upwardly transposed and some slight curvature introduced into the log log plot (inset). (B) The effect of a concentration-dependent mode of monomer denaturation on the reversibly polymerizing system is complex. A faster rate of the second aggregation reaction leads to behavior reminiscent of that seen for the first order denaturation mechanism. ($K_{DEN}=0.1$, Red lines $k_{*+}=17.5$ M^{-1} s^{-1}, blue lines $k_{*+}=87.5$ M^{-1} s^{-1} and black lines original stable case for comparison).

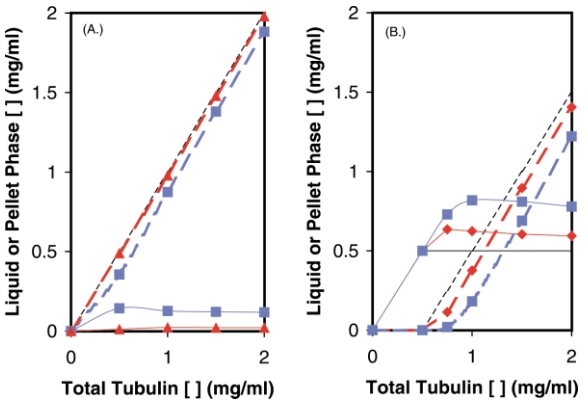

Fig. 12. Effect of denaturation of Tubulin monomer by a concentration-dependent mechanism on the thermodynamic characterization of polymerization profiles. Dashed lines represent microtubule phase, solid lines represent monomer phase. All simulated data points refer to the maximum value obtained from the polymerization profile recorded in Fig. 11. Concentration-dependent denaturation leads, respectively, to artificial estimates of the critical concentration of 0.01 ($\pm$0.005) mg/ml and 0.15 ($\pm$0.01) mg/ml for the (A) irreversibly polymerizing system and 0.64 ($\pm$0.01) and 0.77 ($\pm$0.11) mg/ml for (B) reversibly polymerizing system (the two estimates, respectively, corresponding to the low and high estimates of the denaturation rate). ($K_{DEN}=0.1$, Red lines $k_{*+}=17.5\ M^{-1}\ s^{-1}$, blue lines $k_{*+}=87.5\ M^{-1}\ s^{-1}$ and black lines original stable case for comparison).

imparts marked curvature to the double logarithmic plot shown in the inset.

Fig. 12A and B, respectively, describe the simulated thermodynamic characterization of irreversibly and reversibly polymerizing systems in which the denaturation rate is second order in Tubulin concentration. For the irreversible case, we observe that the presence of a slow rate of denaturation leads to an empirical assessment of 0.01 ($\pm$0.005) mg/ml ($R^2=1.0$, slope = 0.99) for the critical concentration. A fast rate of denaturation yields an apparent critical concentration of 0.15 ($\pm$0.01) mg/ml ($R^2=1.0$, slope = 1.02). The phenomenological critical concentration value inferred from the maximum of the simulation for the reversible case with the slow denaturation rate was 0.64 ($\pm$0.01) mg/ml ($R^2=1.0$, slope = 1.03). The critical concentration inferred from the maximum of the reversible case with the faster denaturation rate was 0.77 ($\pm$0.11) mg/ml ($R^2=1.0$, slope = 0.98).

For the irreversible system (Fig. 13A), we observe only minimal departure of the observed slope of the double logarithmic plot from that of its unperturbed value of 3.0, the slope changes to 2.99 ($\pm$0.02) and 3.11 ($\pm$0.03) for the slow and fast denaturation rate cases, respectively. The change in slope for the effect of denaturation on the reversible case (Fig. 13B) is somewhat greater, the negative value of the slope increases to 4.75 ($\pm$0.38) and 5.52 ($\pm$0.59) for the slow, and fast denaturation rate cases, respectively, from its limiting value of 4.21 predicted for completely stable Tubulin.

In Fig. 14, we examine the effect of a second order decay mechanism on the determination of the growth rate constant of irreversibly (Fig. 14a) and reversibly (Fig. 14b) polymerizing systems. For the irreversible system, evaluation of the slope of the limiting linear portion of each line on the pseudo-first-order rate plot and subsequent combination with the apparently stable number concentration of microtubules provides us with an

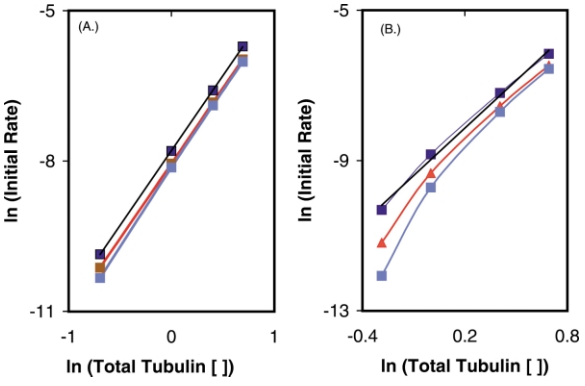

Fig. 13. Effect of denaturation of Tubulin monomer by a concentration-dependent mechanism on the characterization of the lag phase kinetics. (A) Irreversibly polymerizing system. Increasing the denaturation rate has a very slight effect on the slope of the log log plot of initial rate vs. total Tubulin concentration leading to estimates of 2.99 ($\pm$0.02) and 3.11 ($\pm$0.03) for the apparent nucleus size. (B) Reversibly polymerizing system. The effect of increasing the denaturation rate upon the reversible system leads to estimates of 4.75 ($\pm$0.38) and 5.52 ($\pm$0.59) for the two denaturation rate estimates. ($K_{DEN}=0.1$, Red lines $k_{*+}=17.5\ M^{-1}\ s^{-1}$, blue lines $k_{*+}=87.5\ M^{-1}\ s^{-1}$ and black lines original stable case for comparison).

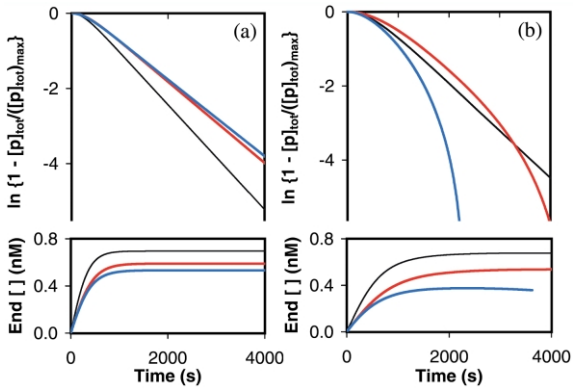

Fig. 14. Effect of denaturation of Tubulin monomer by a concentration-dependent mechanism on the characterization of the growth phase kinetics. The effect of having an initial equilibrium between native and unfolded monomer followed by an irreversible aggregation step introduces complexity into the characterization of the growth kinetics. (a) For the 1.0 mg/ml irreversibly polymerizing system we see that the effect is to decrease the negative value of the slope whilst also decreasing the molar concentration of polymers. These compensatory effects result in relatively unchanged estimates of the growth rate constant of $k_{G+}=1.83\times10^{6}$ M^{-1} s^{-1} (slow denaturation rate) and $k_{G+}=1.89\times10^{6}$ M^{-1} s^{-1} (fast denaturation rate), (b) For the 1.0 mg/ml reversibly polymerizing system we note first a decrease in the apparent negative value of the slope followed by an increase. The asymptotic limit yields estimates of $k_{G+}=6.12$ $(\pm0.05)\times10^{6}$ M^{-1} s^{-1} (slow denaturation rate) and $k_{G+}=1.83$ $(\pm0.04)\times10^{7}$ M^{-1} s^{-1} (fast denaturation rate). Input values $K_{DEN}=0.1$, Red lines $k_{*+}=17.5$ M^{-1} s^{-1}, blue lines $k_{*+}=87.5$ M^{-1} s^{-1} and black lines original stable case for comparison, $k_{G+}=2\times10^{6}$ M^{-1} s^{-1}).

estimate of the association growth rate constant for the more slowly denaturing system of $k_{G+}=1.83$ $(\pm0.00003)\times10^{6}$ M^{-1} s^{-1} [slope (3000–4000 s) $=0.00108$ $(\pm2\times10^{-8})$ s^{-1}, $[E]_{1\ mg/ml}=0.59$ nM]. In a similar fashion, a value of $k_{G+}=1.89$ $(\pm0.00003)\times10^{6}$ M^{-1} s^{-1} [slope (3000–4000 s) $=0.00101$ $(\pm2\times10^{-8})$ s^{-1}, $[E]_{1\ mg/ml}=0.53$ nM] for the system coping with a more rapidly decaying Tubulin monomer. One thing that should be noted about the first order transform of the irreversible growth kinetics shown (Fig. 14a) is that both of the cases exhibiting definite denaturation rates of monomer show limiting slopes that are lower in absolute magnitude than that for the stable case. This is in sharp contrast to the corresponding observation of the reversible case (Fig. 14b) for which we see a steeper limiting behavior. Analysis of the limiting behavior in Fig. 14b yields estimates of $k_{G+}=6.12$ $(\pm0.05)\times10^{6}$ M^{-1} s^{-1} (relatively slowly denaturing system, slope (3500–4000 s) $=0.00328$ $(\pm3\times10^{-5})$ s^{-1}, $[E]_{1\ mg/ml}=0.54$ nM) and $k_{G+}=1.83$ $(\pm0.04)\times10^{7}$ M^{-1} s^{-1} [relatively quicker denaturing system, slope (1800–2200 s) $=0.00682$ (±0.00014) s^{-1}, $[E]_{1\ mg/ml}=0.37$ nM].

For both the irreversible (Fig. 15A, Tubulin concentration $=1$ mg/ml) and reversible (Fig. 15B, Tubulin concentration 1.5 mg/ml) polymer-

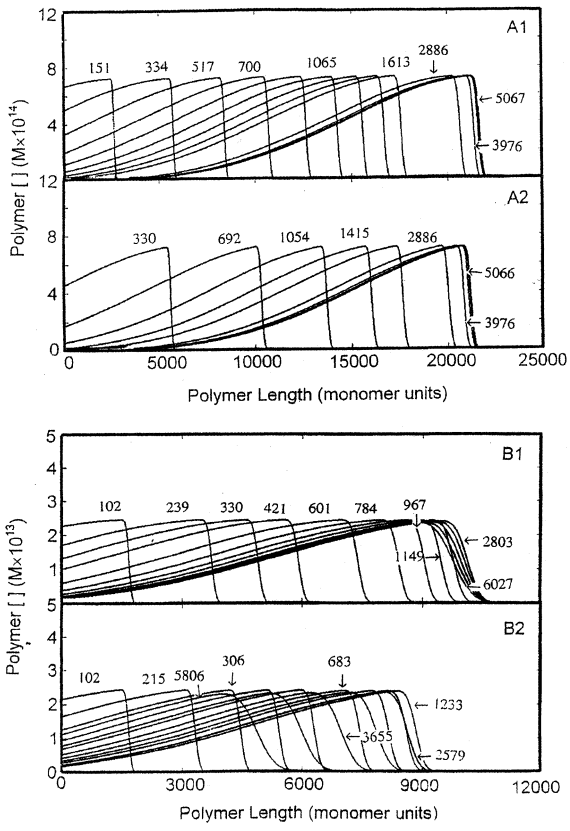

Fig. 15. Examination of the effect of denaturation of the Tubulin monomer by a concentration-dependent mechanism on the kinetics of the microtubule polymer length distribution (A) Length distribution of the 1.0 mg/ml irreversibly polymerizing sample at low (A1) and high denaturation rates (A2). (B) The 1.5 mg/ml reversibly polymerizing sample at the low (B1) and high denaturation rates (B2). Arrows indicate time that the distribution snapshot was taken.

ization modes the effects of a concentration-dependent denaturation mechanism on the time evolution of the distribution are similar to those observed for the first order decay mechanism in the previous section. The only notable exception being that the decrease in the concentration of active Tubulin (due to the rapid equilibrium between M and M^*) requires that the rate of nucleation is decreased resulting in a much lower molar concentration of polymers and therefore necessarily fewer polymers capable of being extended.

4. Discussion

In this simulation study we have examined the effect of two dynamic modes of Tubulin denaturation on the phenomenological kinetic and thermodynamic characterization of the microtubule polymerization reaction. On the basis of our simulations we have suggested that: (i) a significant loss of polymerizable competent Tubulin might occur over the time course of the reaction; and (ii) this loss of active Tubulin, if not recognized, could distort both the qualitative assignment of the system (as either a reversible or irreversible process) and the quantitative estimation of the pertinent kinetic and thermodynamic constants that characterize the system. As this work is simulation based however, the usefulness of the predicted behavior is determined by the basic correctness of our reaction model and chosen parameter estimates.[6] Therefore, in this section we critically examine the strengths and weaknesses of both, the published literature on which this work is based and the extent to which we preserve the physical reality upon transforming the experimental observations into mathematical relations. After establishing the level of trustworthiness of our simulations we then comment on the findings of this work.

4.1. Simplistic description of the polymerization mechanism

In starting out the discussion it is useful to consider the veracity of treating the Tubulin polymerization reaction as a simple nucleated polymerization scheme. Perhaps the greatest uncertainty surrounding the Tubulin polymerization process involves the nucleation event. Various kinetic formulations of the stepwise mechanism used in this study have been suggested including rapid pre-equilibrium [15] and steady state approximations [19,35]. Additionally, more complex mechanisms dependent upon bi-nucleation [16,18] or continuous nucleation [44] models have been used. However, by variation of the nucleus size and rate constants at each stage of the simple stepwise nucleation mechanism adopted in this study most of major types of different conceivable limiting kinetic behaviors for the nucleation event can be reproduced.[7] By choosing our parameter values within confined boundaries we have focused on what we think is the most likely limiting parameter regime in this study. However, we argue for the applicability of our findings to situations involving other conceivable parameter selections in a parameter defense section below.

A noted consequence of the intrinsic polarity of the microtubule structure [46,47] is the existence of a fast growing end (termed the $+$end) and a slow growing end (the $-$end). This property of microtubules under steady state conditions is the physical basis behind the 'treadmilling' phenomenon [47], a process involving sequential passage of Tubulin incorporated into a microtubule from the $+$end to the $-$end while the microtubule maintains a constant length. In light of this behavior, our selection of a single set of rate constants describing addition and dissociation of Tubulin monomer should be appreciated as representing 'averaged' values as would be measured by an experimenter using a non-discriminating technique such as turbidity measurements. It has also been demonstrated that Tubulin, once incorporated into the polymer state, hydrolyses the GTP cofactor at the E site on the β-subunit to form GDP and inorganic phosphate [11]. The GDP-Tubulin complex once formed in the microtubule has a lower affinity for the microtubule state than does GTP-Tubulin [48]. This alteration of the affinity during the residence time of Tubulin in the microtubule

[6] In an appendix we look at the numerical error associated with solving the equations constituting the reaction model.

[7] Manuscript in preparation Hall and Minton, 2003.

state adds an increased level of complexity to the dynamics of the microtubule polymer resulting in intermittent rapid depolymerization and growth phases for individual microtubules. Such behavior, known as dynamic instability, was first proposed by Mitchison and Kirschner [49] and first demonstrated using video microscopy by Horio and Hotani [50]. Studies such as these have provided evidence that the simple behavior predicted for an ensemble average does not adequately describe the kinetic behavior of an individual microtubule. The general phenomena treated in the present paper have been concerned, however, with experimental studies of an assembly of microtubules. With some minor dissent, the broad thrust of experimental investigations over the last 30 years, when concerned with the study of a population of microtubules, have been in fair agreement with a nucleation—growth mechanism similar to that used in this study. It is to investigations of such ensemble averages that this current effort is directed. This is our justification for using such a modeling approach.

4.2. Analysis of the Tubulin denaturation literature

As shown by Table 1, there are many different means for monitoring the denaturation of Tubulin. If the denaturation of Tubulin were to follow the classical 'all or nothing' cooperative two state model of protein folding [51] then there would be no inconsistency with treating all markers of denaturation as equivalent. The situation with Tubulin is more complicated however for the following two reasons: (i) Tubulin can reversibly self assemble to form higher order structures [3,52,53] which may have a different susceptibility to denaturation; and (ii) the denaturation of the Tubulin 'monomer' is believed to occur not by a one step equilibrium but perhaps by a multi-state equilibrium followed by irreversible processes [21–23,45]. In this section, we review the evidence behind these assertions which are key to the simulation model used in this study.

4.2.1. Evidence for instability of the Tubulin monomer

From a theoretical standpoint, it could be argued that the Tubulin monomer would have far greater restrictions on the range of its translational, rotational and vibrational (intra-subunit) motions when present in the polymer state compared to that which it would have when free in solution. This restriction of motion is due to the bonding contact forces that are exerted on a Tubulin molecule by its neighboring Tubulin molecules in the polymer. Indeed for a crystal to form requires the enthalpy of crystallization to have a large enough negative value to overcome the loss in monomer entropy associated with its incorporation into the relatively immobile crystal phase[8] [54]. Support for this argument is provided by common Tubulin experimental practices, such as the thermal cycling procedure for the purification of Tubulin [13,40] and the removal of inactive Tubulin immediately prior to use by a quick cycle of heat-induced polymerization, isolation of the pellet, cold-induced depolymerization, cold high speed centrifugation and subsequent isolation of the supernatant [14,16]. Additionally, storage at very high concentrations is favored, as under these conditions Tubulin is noticeably more stable. Such high concentration conditions are also known to favor oligomer or polymer formation [3,52,53].

4.2.2. Evidence for Tubulin denaturation as a multi-step process

The first identifiable property of active Tubulin was its ability to bind colchicine [55]. For many years, this capability was tacitly assumed to show that Tubulin was in its native form [30,56]. However, further study revealed that the colchicine binding ability of Tubulin is lost at a different rate to its polymerization capability [25]. A possible rationale of this effect was provided by the observation that colchicine may induce a local unfolding of Tubulin [57], a result that possibly indicates colchicine may also be able to bind to partially unfolded Tubulin that is no longer capable of

[8] This is quite a simplistic viewpoint in the sense that we are not discussing the system entropy of the crystallization process. If sufficient bound counter ions and water molecules were liberated upon crystallization then this would compensate somewhat for the loss in entropy of the monomer. Additionally if the excluded volume component of the system was high then the system may minimize entropy losses by polymerizing the macro-molecular component (see [66]).

polymerization. In support of this conclusion was the experimental demonstration that Tubulin exposed to mild urea concentrations (<1.0 M) has an enhanced colchicine binding activity[9] [23]. In addition to the disparity between colchicine binding ability and polymerization ability it has been found that these two markers of Tubulin's 'native' structure are not necessarily lost in a manner coincident with the rate of disappearance of other properties associated with native Tubulin such as its circular dichroism spectra, its fluorescence spectra and its dye binding ability [22]. Findings such as these, in addition to their own work, led Sackett et al. [23] to suggest that Tubulin denaturation may occur via a multi-step process where the distinctive measurable characteristic of Tubulin might be confined to a particular region of protein fold. Local unfolding would lead to a loss of the distinctive characteristic associated with that particular region. By application of different urea concentrations in conjunction with the conduct of a broad spectrum of measurements of the native state of Tubulin, these researchers determined an inequality for relative susceptibility of the marker of Tubulin activity to denaturant concentration, rate of polymerization $>$ extent of polymerization $\sim$ GTPase activity $>$ colchicine binding activity $\sim$ proteolysis by trypsin, chymotrypsin $>$ fluorescent dye binding. Support for the general concept of a local unfolding model for Tubulin has come from urea [45] and thermal unfolding [32] studies, which have implicated a stable intermediate in the unfolding pathway having characteristics of a molten globule [58].

As mentioned above, a complicating factor in the study of Tubulin unfolding is the tendency for Tubulin to reversibly self associate, hence possibly introducing a marked concentration dependence into the estimation of its stability. However, in addition to the reversible association of native Tubulin is the tendency for denatured Tubulin to form irreversible disulfide linked aggregates [21,22,59]. Careful study of the irreversible aggregation process at low temperature (4 °C [21,22,60,61]) has revealed that it is not preventable by inclusion of disulfide reducing agents in solution, thereby suggesting that the sulfhydryl groups involved in the formation of crosslinks in the aggregate species are not exposed to the solvent and react after an association between Tubulin molecules. That such an intimate association can take place between both two denatured Tubulin molecules and also native and denatured Tubulin molecules, has been neatly demonstrated by Maccioni [42] through gel filtration experiments. The size of the irreversible aggregate formed at low temperature has been estimated to be approximately 7 Tubulin dimers [59]. At higher temperatures, this size is not as well determined but it may be that the aggregates are larger and more polydisperse based on evidence gained from non-denaturing gels [60,61] and the fact that irreversible aggregates can often be retrieved from the pellet phase when centrifuging microtubule/Tubulin mixtures [16,24].

On the basis of the preceding evidence, a number of groups have suggested [41] or outlined [21,23,45] mechanisms of Tubulin denaturation similar to Eq. (8) in that they all involve an initial equilibrium followed by an irreversible aggregation process. The partly reversible nature of the process has been established by experiments showing the rapid, but partial, recovery of a native marker of Tubulin when a preservative agent[10] such as D_2O [21] is added to solution, or alternatively when a denaturing agent is removed from solution [45].

In our modeling strategy, we have treated the denaturation mechanism as either a first order process (Eq. (7)) or a rapid equilibrium followed by an irreversible second order aggregation process (Eq. (8)). The decision to include the simple first order case was made for the following two reasons: (i) the use of a one parameter denaturation model allowed us to explore parameter space with less ambiguity than that associated with a more realistic class of model such as that represented by Eq. (8); and (ii) there exists some experimental evidence showing that the loss of Tubulin polymerization

[9] However, this interpretation has been questioned by another set of investigators on the basis of a different technique [45].

[10] An agent that presumably shifts the denaturation equilibrium back to the more native form.

capability can be adequately described by a first order process [22,31,41]. Indeed some limiting cases of Eq. (8) will collapse to yield a pseudo-first-order mechanism analogous to Eq. (7), therefore the two models are not mutually exclusive. Because of the lack of firm parameters for the second order denaturation model represented by Eq. (8), we have made a best estimate of the value of the reversible equilibrium constant between forms competent and incompetent to polymerize. On the basis of experiments that suggest that the initial equilibrium is rapid and relatively large [21,45] we have assumed that the initial reversible equilibrium is instantaneous and governed by a sizable equilibrium constant ($K_{DEN}=0.1$). We admit that the model predictions based on the general reaction model of Eq. (8) should be treated with far greater skepticism because of our lack of more certain input parameters and our inability to fully explore the parameter space due to an increased number of parameters in the model. We decided to include the results of this model as they have the potential to offer, in our opinion, a more realistic view of the system.

4.2.3. Relevance of reported Tubulin denaturation studies

The risk of undertaking a simulation venture such as the present one looking into the effects of Tubulin denaturation on the characterization of the polymerization reaction is that, unlike for the case of a truly independent process (for instance radioactive decay), we cannot divorce the rate of Tubulin denaturation from its solution environment. Obviously we could increase the extent to which the denaturation of Tubulin affects the polymerization time course by changing the solution conditions for the worse (e.g. include denaturing agents in solution [23]), or conversely we could attempt to minimize, experimentally, the effects of denaturation by addition of preservative agents and use of optimal pH, temperature and ionic strength conditions [24,36,37]. Additional permutations arise when one considers that Tubulin sources are many and varied with the purification and isolation from the brain tissue of animals as diverse as Antarctic fishes, cows [40], pigs [12] and rats [62]. Additionally, the Tubulin molecule is known to undergo a number of post-translational modifications which include removal of tyrosine side chains, palmitoylation, glutamylation and phosphorylation [63]. Also, the Tubulin component is often not the sole protein component with experiments commonly being performed on microtubule protein i.e. Tubulin plus a $\sim$20% by weight fractional component of microtubule associated proteins [38]. It is, therefore, important to note that, the reported studies of the rate of Tubulin denaturation which form the core of our simulations, were carried out in solution conditions relevant to present practices in the wider field of Tubulin investigation. Most notably, the recent study by Chakrabarti et al. [21] was carried out at 37 °C at pH 6.9 in 0.1 M PIPES, 1 mM $MgCl_2$, 0.1 mM EGTA, 1 mM GTP—a standard solution condition in modern day microtubule experimentation.

4.2.4. Dependence of simulated results on chosen parameter values

As we have not systematically explored parameter space within the bounds of our basic reaction model (or alternative more complicated reaction models), the question exists as to whether our findings are a feature of the model and therefore necessarily dependent on the particular values of the parameters chosen. The previous sections have presented a line of evidence showing the basic reaction model to be reasonable thereby reducing the question to whether or not the general conclusions are overly sensitive to the choice of input parameters. As the selection of the growth and denaturation rate constants was confined by experimental evidence perhaps most vulnerable to question are the simulation parameters chosen to describe the nucleus size and nucleation rate constants. As for the question of nucleus size, we note that by making the nucleus larger we are also making the critical nucleus more sensitive to subtle changes in viable monomer concentration (i.e. $[N_i] \propto [M]^i$). Therefore by making our case with a nucleus size of 3 we are actually de-emphasizing the effects of denaturation on the polymerization kinetics. The chosen set of nucleation rate constants [$k_{N+}=5000\ M^{-1}\ s^{-1}$, $k_{N-}=500\ s^{-1}$] fall in a parameter regime that allow for a fair descrip-

tion of the concentration of nucleus and pre-nucleus (N_2) over the time course of the polymerization assay in terms of the pre-equilibrium approximation [15]. Therefore, one would expect little change to the observed kinetics and subsequent predicted effects of denaturation if the nucleation rate constants were to increase in magnitude as they would still lie in the pre-equilibrium approximation range. If the nucleation association rate constants were decreased by a few orders of magnitude then the nucleation phase of the reaction would become kinetically rate limited making the pre-equilibrium assumption no longer a suitable approximation. However, the effect of a kinetically rate limiting parameter regime would not alter the broad thrust of most of the outlined effects of denaturation on the phenomenological characterization strategies demonstrated for the following reasons. (i) The effect of denaturation on the thermodynamic characterization is, to a large extent, independent of the rate constants defining the nucleation phase as it depends on the concentration of free monomer. (ii) The effect of denaturation on the characterization of the growth kinetics results from a decreased polymer number concentration (produced by decay of monomer for any parameter regime) and the rate of polymerization during a period of zero nucleation rate (therefore again independent of the nucleation parameters). (iii) The general trends shown for the time evolution of a polymer distribution shrinking because of monomer denaturation would be unaffected by a kinetically limited nucleation association rate. (iv) Although a polymerization reaction defined by a kinetically rate limited parameter set may confound analysis of the initial rate kinetics via a log log plot in the presence and absence of denaturation, the effect of monomer decay will always be to slow the nucleation rate and therefore will always be greater at lower concentrations as they inherently enter the polymer phase more slowly.

As a final answer to this question it should be appreciated that many of the findings of this study are independent of the parameter values chosen and hence are useful as diagnostic tools. For example, denaturation of monomer will produce a reduced polymerization maximum for an irreversible system or a reduced and unstable maximum along with the concomitant shortening of the polymer length distribution as Tubulin leaves the polymer 'phase' for a reversible system.

4.3. Implications of this simulation study

The present study has highlighted some possible effects of dynamic denaturation of Tubulin on the analysis of its polymerization. A key prediction was an apparent increase in slope of the log of initial rate vs. log of total Tubulin concentration (from which the nucleus size can be inferred) when significant denaturation is occurring on the time scale of the polymerization reaction. In this regard, it is interesting to note a recent study [64] that has examined the Tubulin polymerization time course by the technique of filter binding. The experimental design was such as to have no additional GTP in solution, therefore, the system might be expected to have a number of features relevant to the present discussion. It would be predicted [48] that the GTP in the exchangeable site on the β-subunit would partition between the solution and Tubulin bound phases prior to assembly thereby leaving a pool of GTP-Tubulin and nucleotide free Tubulin at a ratio determined by the equilibrium binding constant of Tubulin for GTP. This point is relevant to discussion of the present work as it is known that Tubulin is markedly less stable in the absence of GTP [48]. The second point relative to our discussion is that due to the lack of excess GTP in solution, the hydrolysis of GTP to GDP (known to occur at some stage during polymerization) will result in both Tubulin GDP and additional nucleotide free Tubulin that are not be competent to assemble. Although this mode of loss of assembly competency is not the type that we have considered, it has many features that resemble the dynamic decay central to the thesis of this paper, for instance, the monomer will lose assembly competency over the time scale of the reaction. We see that the experimental time course of Tubulin polymerization in the study by Caudron et al. [64] mimics somewhat those predicted in Figs. 3 and 10 of the present study (to be fair to the authors, however, the denaturation event is definitely not the first or

second order events assumed in this study). A remarkable feature of the study by Caudron et al. [64] was the inconsistency of the estimate of the power dependence of nucleation rate on the Tubulin concentration (gained from a log log plot similar to Figs. 6 and 13 of this study) with the experimentally observed time dependence of the polymer number concentration. This observation led the authors to suggest that the rate of nucleation of the microtubule polymerization reaction was not affected by changes in the concentration of free Tubulin from its initial value. If the reader accepts the relevance of the current simulation study to the results of Caudron et al. [64], then we could suggest that the initial estimate of the power dependence of the initial rate upon Tubulin concentration may have been artificially high due to both, the intrinsic overestimation that accompanies the reversibility of the system, as well as to the continual increase in non-viable Tubulin through the polymerization time course. If the value of the concentration exponent was revised downwards, as is suggested by the current study, then the two lines of experimental evidence presented by Caudron et al. would not seem mutually inconsistent, and therefore, there would be no need for the authors to suggest a new mechanism of microtubule nucleation.

Another interesting feature of the present study was the dependence of the apparent growth rate constant on the rate of denaturation. Increases in the denaturation rate for both modes of denaturation led to an estimate of the growth rate constant nearly 2 orders of magnitude greater than the input value. This observation potentially provides another reason for the disparity of estimates in the literature of the growth rate constant for Tubulin polymerization[11] [33]. The concentration-dependent denaturation mechanism caused the polymerization time course to exhibit apparently biphasic growth kinetics. Such biphasic growth kinetics have been observed [65,66] and attributed to the addition of oligomers to the growing microtubule ends [65] or alternatively explained as an artifact of the measurement process [66]. Our prediction of apparent biphasic growth kinetics brought about by denaturation, provide a simple explanation of such phenomenon. A general conclusion of the study was the increased effect of denaturation on: (i) experiments for which Tubulin polymerization was slow (i.e. those at the lowest concentrations); and (ii) polymerizing systems having a higher intrinsic critical concentration. These findings stemmed directly from the starting assumption that the monomeric form of Tubulin was less stable than the polymeric form. If true, this observation leads one to suggest that for a system having a certain critical concentration, the most reliable data would be that gained from experiments with the highest concentrations of Tubulin and the least reliable data that gained at the lowest concentrations. Such a finding puts a requirement on the experimenter to use both upper and lower concentration bounds to establish the stability of Tubulin over the time scale of the experiment. Use of the highest concentration only could potentially lead the experimenter into erroneously discounting the effect of Tubulin denaturation on the characterization process. In addition, it is important to record data well beyond the attainment of a polymerization maximum to establish either confidence in the time independence of the recorded maximum or alternatively to gather information on the extent to which denaturation may be affecting the system.

In our simulations, we have had the luxury of being able to discriminate between microtubule polymer, native monomer, denatured monomer and low degree disulfide linked irreversible aggregates. We assumed all denatured forms of Tubulin are indistinguishable and do not contribute to the measured signal produced by the microtubule polymer. In reality, the situation is complicated by the fact that whereas denatured monomer would not, some irreversibly linked aggregates may contribute to the measured property (whether it be the amount of pelleted protein or scattered light), therefore, judgment needs to be applied when adapting the general arguments made here to a particular experimental regimen.

5. Concluding remarks

In order for the comparison of results, we often parameterize the behavior of the system under

[11] That interestingly enough cover 2 orders of magnitude.

investigation. Sometimes the parameterization process is based on solid mechanistic grounds whereas at other times it is purely phenomenological in nature. Others have demonstrated that the loss of Tubulin's ability to polymerize may be significant over the time course of a characterization experiment. We have demonstrated that the effects of this denaturation have the potential to distort the parameterization of the system, if not incorporated into the analysis or eliminated experimentally. This study has relied upon numerical solutions to differential equations with specific parameter sets—an approach which obviously lacks the power of a general analytical solution. However, we feel that by pointing out the general form of the distortion introduced by denaturation, the results presented in this work, may aid somewhat, in the reconciliation of conflicting estimates of nucleus size, critical concentration and kinetic rate constants that have arisen in the arena of Tubulin investigation.

This study has important ramifications for the in vitro trial of the effects of new compounds on Tubulin polymerization behavior. If the general mechanism of polymerization remains unchanged then the effect of the added test component may be to either influence the rate or equilibrium constants governing the polymerization process or alternatively it may manifest its effect through altering the intrinsic stability of Tubulin [26,27]. It is only through a firm understanding of how the different processes affect the phenomenological classification of the system that we will be able to get a true idea of the mode of action of the compound in question.

Acknowledgments

Initially I would like to express my thanks to German Rivas who spent a month teaching me how to experiment with Tubulin. I would also like to thank the following people for helpful discussion: Jan Wolff, Dan Sackett, Kenji Sasahara, Herman Edskes, Peter McPhie, Leslie Knipling, P.J. Britto and Allen Minton. Special thanks to my supervisor (Allen Minton) for the support and encouragement shown whilst working in his lab. Finally, I would like to acknowledge the financial assistance provided by the U.S. government in the form of a Fogarty Visiting Fellowship.

Appendix A: Basis of computer model

In the belief that the equations for calculation are sufficiently outlined above in Section 2, this appendix will concentrate on the computing methods that make discrete calculation of the large polymer arrays possible.

A.1. Temporary storage

Initially a $p \times 1$ dimensional array is made for storage of the concentrations of polymer of length $n+$row index to p (where n is the critical nucleus size). A number of 1×1 dimensional arrays are set aside for the storage of the concentrations of monomer, various nuclei species and the final concentration of polymer termed P_{end}. All of these arrays (including the polymer arrays) have a mirror array (same size) that will store their concentration time derivatives for each time point. It should be noted that all the arrays described so far are temporary storage arrays in that same array will take on new values for every time point with the old values being lost upon replacement by the new. A number of non-temporary storage arrays will also be created of dimensionality $1 \times$(number of time increments) that will store the concentration time data of nuclei, monomer and total monomer in polymer. Note, that we will not have a permanent storage array for the distribution of polymer species with time.

A.2. Frame-shifting of polymer array within time increment loop

Imagine a loop that regulates the passage of time. With each cycle of the loop we increase the time by some incremental value Δt. For each cycle we calculate the concentration time derivative for each species from the relevant rate equations. For the polymer species this involves utilizing values preceding and post the row index of each particular species. Instead of writing a sub-loop that goes through and solves for each species i by using the value of $i-1$ and $i+1$ we have utilized the matrix row delete and matrix join statements to create two frame shifted matrices for the polymer of

identical dimensionality so that we can calculate the concentration time derivatives using a matrix approach to speed the process. The backwards frame shifted polymer matrix ($\boldsymbol{P}_{bs}$) has the concentration of $\boldsymbol{P}_{i+1}$ species concentration on the same row index as the $\boldsymbol{P}_i$ value in the original $\boldsymbol{P}$ matrix. Similarly the forwards frame shifted array $\boldsymbol{P}_{fs}$ has the concentration of the $\boldsymbol{P}_{i-1}$ species on the same row index has the $\boldsymbol{P}_i$ species. The principle is demonstrated pictorially:

$\boldsymbol{P}=b \quad \boldsymbol{P}_{bs}=c \quad \boldsymbol{P}_{fs}=a$

$c \qquad d \qquad b$

$d \qquad e \qquad c$

$e \qquad f \qquad d$

therefore the concentration time derivatives can be calculated using

$$d\boldsymbol{P}/dt = -k_{G+}[M]\boldsymbol{P} - k_{G-}\boldsymbol{P} + k_{G-}\boldsymbol{P}_{bs} + k_{G+}\boldsymbol{P}_{fs}[M]$$

A.3. Recycling of initial conditions allows continual adjustment of the size of P Array

Rather than initially having a $\boldsymbol{P}$ array of say, 10,000 species, we start off with an array of say 100, and join a zero matrix onto the end of the $\boldsymbol{P}$ array as is required. This is allowable as the concentration of the longer polymers beyond the growing front will always be zero. This procedure saves vastly on computing time by not performing calculations using large matrix sizes when not required. To implement this matrix extension procedure we place our initial time loop within a second repetition loop that regulates the number of successive time loops in the cycle. Each time we begin a new cycle of our master repetition loop, we obtain our initial conditions for the differential equations by taking the final matrix values of the last time increment of the preceding repetition loop and inserting it as the initial value for the next cycle of the repetition loop.

Appendix B: Veracity of the numerical solution

In this appendix, we set out to demonstrate the basic correctness of the strategy chosen for the numerical solution of the set of differential rate equations used to approximate the polymerizing Tubulin system.

B.1. Strategy for numerical solution of the ordinary differential equation set

Finding a numerical solution of the set of ordinary differential equations (ODE) representing the growing polymer distribution was not a trivial problem. The ODE set in question, is to some extent 'stiff' in the sense that the time scale required for the solution of the individual members of the ODE set can vary by several orders of magnitude over the length distribution of the growing polymer front. Initial attempts at finding a solution relied upon a fourth order Runge–Kutta numerical integration procedure in which the introduced solution error was monitored and controlled by correcting the integration step so as to keep the relative error for each ODE member within a set tolerance limit. This approach failed because it could not make sufficient headway into the time course of the polymerization reaction—a problem inherent in standard attempts at the solution of a stiff set of ODEs. The problem was overcome, not by moving to more complex numerical solution methods, but instead correcting for solution error within the Runge–Kutta routine by monitoring the relative error associated with a number of whole system properties of the ODE suite and using these in deciding the extent of the step-size modification. The general properties monitored were: (i) the concentration of free monomer at each time step; (ii) the concentration of monomer as polymer; (iii) the concentration of 'ends' capable of supporting polymer growth; and (iv) the concentration of the critical nucleus.

B.2. Monitoring the relative error for the four global properties

The gauging of the introduced solution error based on the change in monomer concentration at each step was effected by simple comparison of the two summations of the approximate solutions

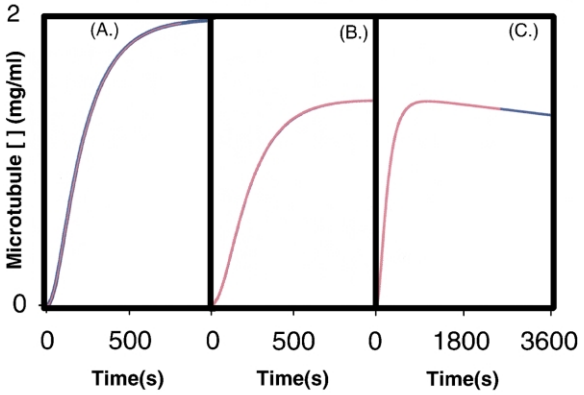

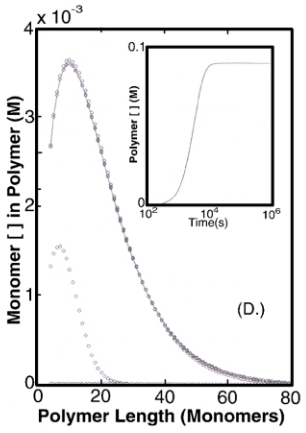

produced within the separate single and double step solutions of the Runge–Kutta algorithm. The correction for solution error based on observation of the concentration of ends at each time point first involved calculating a term by summation of all species of degree equal or greater than the critical nucleus size (from the more accurate double step routine of the Runge–Kutta algorithm). This term was then compared with a more accurate term calculated by the Euler based numerical integration of a single equation describing the rate of formation of all viable ends. This equation was derived from the summation of the total set of rate equations for all species having a degree greater than that of the critical nucleus and was calculated afresh for each time point in the sense that the initial condition was always taken as the concentration of ends calculated by summation of all polymer species and critical nucleus at the start of the prescribed time interval. The potential for the introduction of major solution error exists primarily during the nucleation/end generating phase of the process. The requirement for low relative error of the total concentration of ends and the critical nucleus concentration ensures that this term is accurately calculated. By harnessing the integration step-size to the maximum the four relative errors associated with the concentration of ends, critical nucleus and free and polymerized monomer concentration the ODE suite remained stable at later times when the rate of end generation becomes exceedingly small.

B.3. Demonstration of the basic correctness of the numerical simulation strategy

Demonstration of the basic correctness of the simulation strategy comes from the identity of the irreversible solution for the polymerization time course (Eq. (2)) with that obtained from solving

Fig. A1. Appendix figure 1 (A) Check for numerical error in irreversible solution of the complete set of rate equations—equivalence between solutions for simulation of irreversible polymer formation by the truncated approach (blue line equation set [4]) and the complete solution (pink line equation set [2]) for the following parameter regime: $k_{N+}=5000\ M^{-1}\ s^{-1}$, $k_{N-}=500\ s^{-1}$, $k_{G+}=2\times10^{6}\ M^{-1}\ s^{-1}$, $n=3$, $k_{G-}=0\ s^{-1}$ and $[M]_{tot}=2.0$ mg/ml. (B and C) Check for numerical error in reversible solution of the complete set of rate equations—equivalence between solutions for simulation of reversible polymer formation by two estimates of the complete solution (equation set [2]) having a fourfold difference in the acceptable relative percentage error tolerance allowable between numerical integration steps (pink 2.5 parts in one million, blue 10 parts in one million). (1b) Equivalence over short time and (1c) equivalence over long time. (Parameter regime $k_{N+}=5000\ M^{-1}\ s^{-1}$, $k_{N-}=500\ s^{-1}$, $k_{G+}=2\times10^{6}\ M^{-1}\ s^{-1}$, $n=3$, $k_{G-}=10\ s^{-1}$ and $[M]_{tot}=2.0$ mg/ml, $k_{den}=0.8\times10^{4}\ M^{-1}\ s^{-1}$). (D) Check for correct prediction of the equilibrium position by kinetic simulation—equivalence between solutions carried out using thermodynamic (equation set 3 shown as line) and kinetic approaches [equation set 2 circles at times 0.1, 1272, 50,894 and 550,568 s (see inset)] for a parameter system having a smaller distribution than that simulated in the main text ($k_{N+}=0.001\ M^{-1}\ s^{-1}$, $k_{N-}=0.001\ s^{-1}$, $k_{G+}=0.1\ M^{-1}\ s^{-1}$, $k_{G-}=0.01\ s^{-1}$, $n=3$ and $[M]_{tot}=0.2$ M).

Eq. (4). Equation set 4 has been made 'non-stiff' to a large extent by adoption of the irreversibility constraint prior to the formation of the ODE suite (Fig. A1A). With regards to the reversible system Fig. A1B depicts two separate solutions of a polymerization time course, whereby each solution has a different set relative error tolerance, the total span of error tolerances being a factor of four. As can be noted, any solution with a relative error tolerance of no greater than 10 parts in one million[12] converged to produce a common estimate even when taken over a much longer time scale (Fig. A1C) (the convergence of the solutions having different error tolerances also extending to the length distribution information). Additional evidence for the veracity of the simulation technique can be drawn from the fact that the kinetically calculated end point (for the reversible case) agrees with the predicted equilibrium distribution and end point calculated from thermodynamic considerations (see Fig. A1D).

References

[1] D.L. Sackett, R.E. Lippoldt, Thermodynamics of reversible monomer–dimer association of tubulin, Biochemistry 30 (1991) 3511–3517.

[2] K.W. Wood, W.D. Cornwell, J.R. Jackson, Past and future of the mitotic spindle as an oncology target, Curr. Opin. Pharmacol. 1 (2001) 370–377.

[3] K.E. Shearwin, S.N. Timasheff, Linkage between ligand binding and control of tubulin conformation, Biochemistry 31 (1992) 8080–8089.

[4] J.M. Andreu, S.N. Timasheff, Tubulin bound to colchicine forms polymers different from microtubules, Proc. Natl. Acad. Sci. U.S.A. 79 (1982) 6753–6756.

[5] F. Gaskin, Y. Kress, Zinc ion-induced assembly of tubulin, J. Biol. Chem. 252 (1977) 6918–6924.

[6] E. Nogales, M. Whittaker, R.A. Milligan, K.H. Downing, High-resolution model of the microtubule, Cell 96 (1999) 79–88.

[7] F.J. Medrano, J.M. Andreu, M.J. Gorbunoff, S.N. Timasheff, Roles of colchicine rings B and C in the binding process to tubulin, Biochemistry 28 (1989) 5589–5599.

[8] S.N. Timasheff, J.M. Andreu, G.C. Na, Physical and spectroscopic methods for the evaluation of the interactions of antimitotic agents with tubulin, Pharmac. Ther. 52 (1991) 191–210.

[9] J.F. Diaz, M. Menendez, J.M. Andreu, Thermodynamics of ligand-induced assembly of tubulin, Biochem. 32 (1993) 10067–10077.

[10] R.C. Weisenberg, The role of nucleotide triphosphate in actin and tubulin assembly and function, Cell Motil. 1 (1981) 485–497.

[11] T. David-Pfeuty, Mechanism of GTP hydrolysis at microtubule ends, Biophys. Chem. 12 (1980) 121–131.

[12] F. Gaskin, C.R. Cantor, M.L. Shelanski, Turbidimetric studies of the in vitro assembly and disassembly of porcine neurotubules, J. Mol. Biol. 89 (1974) 737–755.

[13] K.A. Johnson, G.G. Borisy, in: S. InouJ, R.E. Stephens (Eds.), Molecules and Cell Movement, Raven Press, New York, 1975, pp. 119–141.

[14] K.A. Johnson, G.G. Borisy, Kinetic analysis of microtubule self-assembly in vitro, J. Mol. Biol. 117 (1977) 1–31.

[15] F. Oosawa, S. Asakura, Thermodynamics of the Polymerization of Protein, Academic Press, New York, 1975.

[16] W.A. Voter, H.P. Erickson, The kinetics of microtubule assembly. Evidence for a two-stage nucleation mechanism, J. Biol. Chem. 259 (1984) 10430–10438.

[17] M.F. Carlier, D. Pantaloni, Kinetic analysis of cooperativity in tubulin polymerization in the presence of guanosine di- or triphosphate nucleotides, Biochemistry 17 (1978) 1908–1915.

[18] H. Flyvbjerg, E. Jobs, S. Leibler, Kinetics of self-assembling microtubules: an 'inverse problem' in biochemistry, Proc. Natl. Acad. Sci. U.S.A 93 (1996) 5975–5979.

[19] Y. Engelborghs, L.C.M. De Maeyer, N. Overbergh, A kinetic analysis of the assembly of microtubules in vitro, FEBS Lett. 80 (1977) 81–85.

[20] R.G. Burns, Assembly of chick brain MAP2-tubulin microtubule protein. Characterization of the protein and the MAP2-dependent addition of tubulin dimers, Biochem. J. 277 (1991) 231–238.

[21] G. Chakrabarti, S. Kim, M.L. Gupta Jr., J.S. Barton, R.H. Himes, Stabilization of tubulin by deuterium oxide, Biochemistry 38 (1999) 3067–3072.

[22] V. Prakash, S.N. Timasheff, Aging of tubulin at neutral pH, J. Mol. Biol. 160 (1982) 499–515.

[23] D.L. Sackett, B. Bhattacharyya, J. Wolff, Local unfolding and the stepwise loss of the functional properties of tubulin, Biochemistry 33 (1994) 12868–12878.

[24] R.A. Keates, Stabilization of microtubule protein in glycerol solutions, Can. J. Biochem. 59 (1981) 353–360.

[25] J.S. Barton, Polymerization and colchicine binding. Two independent properties of tubulin, Biochim. Biophys. Acta. 532 (1978) 155–160.

[26] V. Prakash, S.N. Timasheff, Arch. Biochem. Biophys. 295 (1992) 146–152.

[27] V. Prakash, S.N. Timasheff, Aging of tubulin at neutral pH: the destabilizing effect of vinca alkaloids, Arch. Biochem. Biophys. 295 (1992) 137–145.

[12] This was relaxed fivefold after the system had surpassed a third of its end point or maximal value.

[28] M.B. Jackson, S.A. Berkowitz, Nucleation and the kinetics of microtubule assembly, Proc. Natl. Acad. Sci. U.S.A. 77 (1980) 7302–7305.
[29] H.J. Hinz, S.N. Timasheff, Enthalpy changes in microtubule assembly from pure tubulin, Biochemistry 25 (1986) 8285–8291.
[30] R.P. Frigon, J.C. Lee, The stabilization of calf-brain microtubule protein by sucrose, Arch. Biochem. Biophys. 153 (1972) 587–589.
[31] M. Menedez, G. Rivas, J. Fernando Diaz, J.M. Andreu, Control of the structural stability of the tubulin dimer by one high affinity bound magnesium ion at nucleotide N-site, J. Biol. Chem. 273 (1998) 167–176.
[32] A. Mozo-Villarius, A. Morros, J.M. Andreu, Thermal transitions in the structure of tubulin. Environments of aromatic amino acids, Eur. Biophys. J. 19 (1991) 295–300.
[33] Y. Engelborghs, Dynamic aspects of microtubule assembly, in: J. Avila (Ed.), Microtubule Proteins, CRC, Boca Raton FL, 1990.
[34] N. Kumar, Taxol-induced polymerization of purified tubulin. Mechanism of action, J. Biol. Chem. 256 (1981) 10435–10441.
[35] A. Wegner, J. Engel, Kinetics of the cooperative association of actin to actin filaments, Biophys. Chem. 3 (1975) 215–225.
[36] P.G. Waxman, A.A. Del Campo, M.C. Lowe, E. Hamel, Induction of polymerization of purified tubulin by sulfonate buffers. Marked differences between 4-morpholineethanesulfonate (Mes) and 1,4-piperazineethanesulfonate (Pipes), Eur. J. Biochem. 120 (1981) 129–136.
[37] J.C. Lee, S.N. Timasheff, In vitro reconstitution of calf brain microtubules: effects of solution variables, Biochemistry 16 (1977) 1754–1764.
[38] J.J. Correia, R.C. Williams Jr., Mechanisms of assembly and disassembly of microtubules, Ann. Rev. Biophys. Bioeng. 12 (1983) 211–235.
[39] F. Gaskin, Techniques for the study of microtubule assembly in vitro, Meth. Enzymol. 85B (1982) 433–439.
[40] M.L. Shelanski, F. Gaskin, C.R. Cantor, Microtubule assembly in the absence of added nucleotides, Proc. Natl. Acad. Sci. U.S.A. 70 (1973) 765–768.
[41] G. Wiche, L.S. Honig, R. David Cole, Polymerising ability of C6 glial cell microtubule protein decays much faster than its colchicine-binding activity, Nature 269 (1977) 435–436.
[42] R.B. Maccioni, Microtubule assembly affected by the presence of denatured tubulin, Biochem. Biophys. Res. Com. 2 (1983) 463–469.
[43] D.L. Purich, T.L. Karr, D. Kristofferson, Microtubule disassembly: a quantitative kinetic approach for defining endwise linear depolymerization, Meth. Enzymol. 85 (1982) 439–450.
[44] R.P. Sear, Homogeneous nucleation of a noncritical phase near a continuous phase transition, Phys. Rev. E. 63 (066105) (2001) 1–5.
[45] S. Guha, B. Bhattacharyya, Refolding of urea-denatured tubulin: recovery of nativelike structure and colchicine binding activity from partly unfolded states, Biochemistry 36 (1997) 13208–13213.
[46] L.A. Amos, A. Klug, Arrangement of subunits in flagellar microtubules, J. Cell. Sci. 14 (1974) 523–549.
[47] R.L. Margolis, L. Wilson, Opposite end assembly and disassembly of microtubules at steady state in vitro, Cell 13 (1978) 1–8.
[48] J.J. Correia, L.T. Baty, R.C. Williams Jr., Mg^{2+} dependence of guanine nucleotide binding to tubulin, J. Biol. Chem. 262 (1987) 17278–17284.
[49] T. Mitchison, M. Kirschner, Microtubule assembly nucleated by isolated centrosomes, Nature 312 (1984) 237–242.
[50] T. Horio, H. Hotani, Visualization of the dynamic instability of individual microtubules by dark-field microscopy, Nature 321 (1986) 605–607.
[51] J.F. Brandts, Conformational transitions of proteins in water and in aqueous mixtures, in: S.N. Timasheff, G.D. Fasman (Eds.), Structure and Stability of Biological Macromolecules, Marcel Dekker, Inc, New York, 1969.
[52] R.B. Vallee, G.G. Borisy, The non-tubulin component of microtubule protein oligomers. Effect on self-association and hydrodynamic properties, J. Biol. Chem. 253 (1978) 2834–2845.
[53] G. Rivas, J.A. Fernandez, A.P. Minton, Direct observation of the self-association of dilute proteins in the presence of inert macromolecules at high concentration via tracer sedimentation equilibrium: theory, experiment and biological significance, Biochemistry 38 (1999) 9379–9388.
[54] T.L. Hill, Linear aggregation theory in cell biology, in: A. Rich (Ed.), Springer Series in Molecular Biology, series Ch. 2, Springer Verlag, New York, 1987.
[55] R.C. Weisenberg, G.G. Borisy, E.W. Taylor, The colchicine-binding protein of mammalian brain and its relation to microtubules, Biochemistry 7 (1968) 4466–4478.
[56] F. Solomon, D. Monard, M. Rentsch, Stabilization of colchicine-binding activity of neuroblastoma, J. Mol. Biol. 78 (1973) 569–573.
[57] D.L. Sackett, J.K. Varma, Molecular mechanism of colchicine action: induced local unfolding of beta-tubulin, Biochemistry 32 (1993) 13560–13565.
[58] O.B. Ptitsyn, R.H. Pain, G.V. Semisotnov, E. Zerovnik, I.O. Razgulyaev, Evidence for a molten globule state as a general intermediate in protein folding, FEBS Lett. 262 (1990) 20–24.
[59] W. Howard, S.N. Timasheff, Quasi-elastic light scattering studies of tubulin aggregation, Arch. Biochem. Biophys. 255 (1987) 446–452.
[60] J.J. Correia, M.K. Welch, R.C. Williams Jr., Evidence for the spontaneous formation of disulfide crosslinked

aggregates of tubulin during nondenaturingelectrophoresis, Arch. Biochem. Biophys. 255 (1987) 244–253.
[61] J.J. Correia, R.C. Williams Jr., Characterization of oligomers of tubulin by two-dimensional native electrophoresis, Arch. Biochem. Biophys. 239 (1985) 120–129.
[62] D.L. Sackett, L. Knipling, J. Wolff, Isolation of microtubule protein from mammalian brain frozen for extended periods of time, Prot. Expr. Purif. 2 (1991) 390–393.
[63] J. Rosenbaum, Cytoskeleton: functions for tubulin modifications at last, Curr. Biol. 10 (2000) R801–803.
[64] N. Caudron, O. Valiron, Y. Usson, P. Valiron, D. Job, A reassessment of the factors affecting microtubule assembly and disassembly in vitro, J. Mol. Biol. 297 (2000) 211–220.
[65] P.K. Smith, R.I. Krohn, G.T. Hermanson, et al., Measurement of protein using bicinchoninic acid, Anal. Biochem. 150 (1985) 76–85.
[66] D.R. Hall, A.P. Minton, Effects of inert volume-excluding macromolecules on protein fiber formation. I. Equilibrium models, Biophys. Chem. 98 (2002) 93–104.
[67] J.J. Coreia, L.D. Lipscomb, S. Lobert, Nondisulfide crosslinking and chemical cleavage of tubulin subunits: pH and temperature dependence, Arch. Biochem. Biophys. 300 (1993) 105–114.
[68] J. Najbauer, J. Orpiszewski, D.W. Aswad, Molecular aging of tubulin: accumulation of isoaspartyl sites in vitro and in vivo, Biochemistry 35 (1996) 5183–5190.